INSTITUTO TECNOLÓGICO DE AERONÁUTICA

Victor Maciel

OPTIMIZATION OF AIRCRAFT SEQUENCING USING MIXED-INTEGER PROGRAMMING

Final Paper
2024

Computer Engineering Course

CDU 629.73.08

Victor Maciel

OPTIMIZATION OF AIRCRAFT SEQUENCING USING MIXED-INTEGER PROGRAMMING

Advisor

Prof. Dr. Carlos Henrique Costa Ribeiro (ITA)

Co-advisor

Prof. Dr. Luís Felipe Bueno (UNIFESP)

COMPUTER ENGINEERING

São José dos Campos
Instituto Tecnológico de Aeronáutica

2024

Cataloging-in Publication Data
Documentation and Information Division

Maciel, Victor
Optimization of Aircraft Sequencing Using Mixed-Integer Programming / Victor Maciel.
São José dos Campos, 2024.
84f.

Final paper (Undergraduation study) – Computer Engineering Course – Instituto Tecnológico de Aeronáutica, 2024. Advisor: Prof. Dr. Carlos Henrique Costa Ribeiro. Co-advisor: Prof. Dr. Luís Felipe Bueno.

1. Pesquisa operacional. 2. Métodos heurísticos. 3. Controle de tráfego aéreo. 4. Aterrissagem. 5. Decolagem. 6. Otimização. 7. Matemática. 8. Transportes. I. Instituto Tecnológico de Aeronáutica. II. Optimization of Aircraft Sequencing Using Mixed-Integer Programming.

BIBLIOGRAPHIC REFERENCE

MACIEL, Victor. **Optimization of Aircraft Sequencing Using Mixed-Integer Programming**. 2024. 84f. Final paper (Undergraduation study) – Instituto Tecnológico de Aeronáutica, São José dos Campos.

CESSION OF RIGHTS

AUTHOR'S NAME: Victor Maciel
PUBLICATION TITLE: Optimization of Aircraft Sequencing Using Mixed-Integer Programming.
PUBLICATION KIND/YEAR: Final paper (Undergraduation study) / 2024

It is granted to Instituto Tecnológico de Aeronáutica permission to reproduce copies of this final paper and to only loan or to sell copies for academic and scientific purposes. The author reserves other publication rights and no part of this final paper can be reproduced without the authorization of the author.

Victor Maciel

Victor Maciel
Rua H8A, Ap. 127
12.228-460 – São José dos Campos–SP

OPTIMIZATION OF AIRCRAFT SEQUENCING USING MIXED-INTEGER PROGRAMMING

This publication was accepted as Final Work of Undergraduation Study

Victor Maciel

Victor Maciel

Author

Prof. Dr. Carlos Henrique Costa Ribeiro (ITA)

Advisor

Prof. Dr. Luís Felipe Bueno (UNIFESP)

Co-advisor

Marcos Ricardo Omena de Albuquerque Maximo

Prof. Dr. Marcos Ricardo Omena de Albuquerque Máximo
Computer Engineering Course Coordinator

São José dos Campos: November 12, 2024.

Aos meus pais, meus maiores incentivadores, que me ensinaram o valor da educação e me apoiaram em todos os momentos ao longo da minha vida. Sem eles, nada disso seria possível.

Acknowledgments

First and foremost, I thank God for illuminating my path and guiding me with wisdom and strength throughout my life. To my parents, Mauro and Patricia, who have always believed in me, investing in my education and providing me with the best opportunities within their reach. To my family, for their unconditional love and constant support, present at every stage of this journey. To my friends Alexandre, Bernardo, Cassia, Rafael and Schultz, for standing by my side at all times, offering encouragement, support, and a friendship that made this journey truly fulfilling. To my advisors, Professors Carlos and Luís, for their unwavering guidance and commitment throughout this work. To all the other professors at ITA, whose dedication to teaching has significantly enriched my learning. To the ICEA staff for their support throughout the year, especially Capitão Melo and Jean. To my classmates from Class 24, whose companionship made this journey lighter and more enjoyable. And to everyone who, in one way or another, contributed to the completion of this work. To all of you, my deepest gratitude.

"Já que é preciso aceitar a vida, que seja então corajosamente."
— Lygia Fagundes Telles, Ciranda de Pedra

Abstract

The rapid growth in global air travel demand has significantly increased air traffic, leading to heightened delays and environmental concerns. This surge underscores the critical need for optimized sequencing techniques in air traffic management to maintain operational efficiency. Operational Research provides powerful methods to tackle these complex issues by offering structured approaches for optimization. In this study, we develop a Mixed-Integer Programming model to address the Aircraft Landing Problem, incorporating operational constraints specific to Guarulhos International Airport. Our model aims to enhance the efficiency of aircraft landing sequences by minimizing cumulative deviations from unimpeded times, thereby reducing fuel consumption and improving overall airport performance. To assess the model's viability and efficacy, we employed a data-driven approach, collecting real operational data from Guarulhos International Airport during select days in 2023. This approach enabled us to evaluate the model under various traffic scenarios, including those involving threshold changes. The results indicate that our model's implementation consistently achieved viable solutions with practical execution times and outperformed both actual operational data and the First-Come, First-Served (FCFS) baseline regarding deviations from unimpeded times. Under clear visibility and moderate traffic conditions, the model showed an average improvement of 93.33% over real data and 29.91% over the FCFS baseline. In peak traffic scenarios, it demonstrated a maximum improvement of 60.15% compared to FCFS when optimization began at 100 nautical miles (NM) from the airport, with an average improvement of 45.37% across the analyzed days. When optimization began at 40 NM from the airport, the model achieved an average improvement of 31.64% over FCFS. Similar gains were observed in scenarios involving threshold changes. These findings demonstrate the model's potential as a robust tool for optimizing landing sequences, contributing to reduced deviations from unimpeded times and environmental impact, while enhancing overall airport efficiency.

Resumo

O rápido crescimento da demanda global por viagens aéreas aumentou significativamente o tráfego aéreo, resultando em maiores atrasos e preocupações ambientais. Esse cenário ressalta a necessidade crítica de técnicas de sequenciamento otimizadas na gestão do tráfego aéreo para manter a eficiência operacional. A Pesquisa Operacional oferece métodos para abordar esses desafios, fornecendo abordagens estruturadas para otimização. Este estudo apresenta um modelo de Programação Inteira Mista para tratar o Problema de Sequenciamento de Pousos de Aeronaves, incorporando restrições operacionais específicas do Aeroporto Internacional de Guarulhos. O modelo busca aumentar a eficiência das sequências de pouso, minimizando os desvios cumulativos em relação aos tempos desimpedidos, reduzindo o consumo de combustível e melhorando o desempenho geral do aeroporto. Para avaliar a viabilidade e eficácia do modelo, foi adotada uma abordagem orientada por dados, utilizando informações operacionais reais coletadas do Aeroporto Internacional de Guarulhos durante dias selecionados de 2023. Essa abordagem permitiu avaliar o modelo em diferentes cenários de tráfego, incluindo aqueles envolvendo trocas de cabeceira. Os resultados indicam que a implementação do modelo obteve consistentemente soluções viáveis com tempos de execução práticos e superou tanto os dados operacionais reais quanto a abordagem *First-Come, First-Served* (FCFS) no que diz respeito aos desvios em relação aos tempos desimpedidos. Sob condições de boa visibilidade e tráfego moderado, a implementação do modelo apresentou uma melhoria média de 93,33% em relação aos dados reais e 29,91% em relação ao método FCFS. Em cenários de pico de tráfego, foi observada uma melhoria máxima de 60,15% em relação ao FCFS, quando a otimização foi iniciada a 100 milhas náuticas (NM) do aeroporto, com uma melhoria média de 45,37% nos dias analisados. Quando a otimização foi iniciada a 40 NM, o modelo alcançou uma melhoria média de 31,64% em relação ao FCFS. Ganhos semelhantes foram observados em cenários com trocas de cabeceira. Esses resultados demonstram o potencial do modelo como uma ferramenta robusta para otimizar sequências de pouso, contribuindo para a redução de desvios em relação aos tempos desimpedidos e de impactos ambientais, além de aprimorar a eficiência operacional do aeroporto.

List of Figures

FIGURE 1.1 – Overview of AMAN System Data Flow (Skybrary, 2024). 18

FIGURE 3.1 – Comparison between the FCFS and the optimal order. 28

FIGURE 4.1 – Example of optimization output. 42

FIGURE 4.2 – Boundaries at 40 (inner circle) and 100 (outer circle) nautical miles centered on Guarulhos Airport. 43

FIGURE 4.3 – Histogram of flights by hour on October 5, 2023. 49

FIGURE 4.4 – Histogram of flights by hour on September 13, 2023. 50

FIGURE 4.5 – Histogram of flights by hour on December 12, 2023. 50

FIGURE 6.1 – KPI08 comparison for January 28, 2023, during the 08:00 to 10:00 period in the C40 scenario. 62

FIGURE 6.2 – KPI08 comparison for March 21, 2023, during the 18:00 to 20:00 period in the C40 scenario. 62

FIGURE 6.3 – KPI08 comparison for April 24, 2023, during the 08:00 to 10:00 period in the C40 scenario. 63

FIGURE 6.4 – Cumulative absolute KPI08 values for January 28, March 21, and April 24, 2023, in the C40 scenario. 63

FIGURE 6.5 – KPI08 comparison for January 28, 2023, during the 08:00 to 10:00 period in the C100 scenario. 65

FIGURE 6.6 – KPI08 comparison for March 21, 2023, during the 18:00 to 20:00 period in the C100 scenario. 65

FIGURE 6.7 – KPI08 comparison for April 24, 2023, during the 08:00 to 10:00 period in the C100 scenario. 66

FIGURE 6.8 – Cumulative absolute KPI08 values for January 28, March 21, and April 24, 2023, in the C100 scenario. 66
FIGURE 6.9 – KPI08 comparison for March 01, 2023, during the 18:00 to 20:00 period in the C40 scenario with threshold change. 68
FIGURE 6.10 – KPI08 comparison for March 29, 2023, during the 15:00 to 17:00 period in the C40 scenario with threshold change. 68
FIGURE 6.11 – KPI08 comparison for May 20, 2023, during the 19:00 to 21:00 period in the C40 scenario with threshold change. 69
FIGURE 6.12 – Cumulative absolute KPI08 values for March 01, March 29, and May 20, 2023, in the C40 scenario. 69
FIGURE 6.13 – KPI08 comparison for March 01, 2023, during the 18:00 to 20:00 period in the C40 scenario with threshold change. 70
FIGURE 6.14 – KPI08 comparison for March 29, 2023, during the 15:00 to 17:00 period in the C100 scenario with threshold change. 71
FIGURE 6.15 – KPI08 comparison for May 20, 2023, during the 19:00 to 21:00 period in the C100 scenario with threshold change. 71
FIGURE 6.16 – Cumulative absolute KPI08 values for March 01, March 29, and May 20, 2023, in the C100 scenario. 72
FIGURE 6.17 – KPI08 values for our model and FCFS model for the C40 scenario on October 5, 2023. 73
FIGURE 6.18 – KPI08 values for our model and FCFS model for the C40 scenario on September 13, 2023. 74
FIGURE 6.19 – KPI08 values for our model and FCFS model for the C40 scenario on December 1, 2023. 74
FIGURE 6.20 – Cumulative absolute KPI08 values for October 5, December 1, and September 13, 2023, in the C40 scenario. 75
FIGURE 6.21 – KPI08 values for our model and FCFS model for the C100 scenario on October 5, 2023. 76
FIGURE 6.22 – KPI08 values for our model and FCFS model for the C100 scenario on September 13, 2023. 76
FIGURE 6.23 – KPI08 values for our model and FCFS model for the C100 scenario on December 1, 2023. 77
FIGURE 6.24 – Cumulative absolute KPI08 values for October 5, December 1, and September 13, 2023, in the C100 scenario. 77

FIGURE 6.25 –Histogram of aircraft categories for the days analyzed in this study. 78

List of Tables

TABLE 4.1 – Separation Requirements in seconds for Landing Aircraft. 47

TABLE 6.1 – Comparison of execution time, value, number of constraints and variables between the Classic Model and Our Model for different values of N and R. 57

TABLE 6.2 – Optimization results for the C40 scenario based on radar data from October 5, 2023, during the 10th hour. 59

TABLE 6.3 – Optimization results for the C100 scenario based on radar data from October 5, 2023, during the 10th hour. 61

List of Abbreviations and Acronyms

IATA	International Air Transport Association
ATM	Air Traffic Management
AMAN	Arrival Manager
ATCOs	Air Traffic Controllers
OR	Operations Research
MIP	Mixed-Integer Programming
ICEA	Airspace Control Institute
ALP	Aircraft Landing Problem
WV	Vortex Turbulence
ICAO	International Civil Aviation Organization
FCFS	First-Come, First-Served
ETA	Estimated Time Arrival
GRU	Guarulhos International Airport
TMA	Terminal Maneuvering Area
METAR	Meteorological Aerodrome Report
KPI	Key Performance Indicator
DECEA	Department of Airspace Control
ICA	Aeronautical Command Instruction
BIMTRA	Air Traffic Movement Information Bank

Contents

1 Introduction 17

1.1 **Motivation** 17

1.2 **Contextualization** 19

1.3 **Objective** 20

1.4 **Literature Review** 20

1.5 **Contributions** 22

1.6 **Outline of the Work** 23

2 Theoretical Background 24

2.1 **MIP: Formulation and Applications** 24

2.2 **Complexity and Challenges of MIP** 25

2.3 **The Fundamental Theorem of Linear Programming** 25

2.4 **The Simplex Method: Efficient Traversal of Vertices** 25

2.5 **Branch-and-Bound and Branch-and-Cut** 26

3 Aircraft Landing Problem 27

3.1 **Main Constraints** 27

3.1.1 Time Window Constraint 27

3.1.2 Minimum Separation Constraint 27

3.2 **Additional Constraints** 29

3.2.1 Priority Aircraft 29

3.2.2 Emergency Aircraft 29

3.2.3 Threshold change 29

3.3 **Classic ALP Model** 30

3.3.1 Parameters . . . 30
3.3.2 Variables . . . 31
3.3.3 Constraints . . . 31
3.3.4 Objective Function . . . 33
3.4 Implemented Model . . . 34
3.4.1 Main Differences . . . 34
3.4.2 Constraints . . . 35
3.4.3 New Constraints . . . 36
3.4.4 Objective Function . . . 39
3.5 Model with Threshold Change . . . 39
4 Methodology . . . 41
4.1 Comparison with the Classic Model . . . 41
4.2 Data Acquisition and Preparation . . . 42
4.2.1 Set of Aircraft and Runways . . . 43
4.2.2 Target landing time . . . 44
4.2.3 Additional Time in the Terminal Area . . . 45
4.2.4 Earliest and latest landing times . . . 46
4.2.5 Minimum Separation Times . . . 46
4.2.6 Data Retrieval Process . . . 47
4.3 Testing the Model . . . 48
5 Detailed Testing Methodology . . . 51
5.1 Feasibility Test . . . 51
5.2 Efficacy without Threshold Change Test . . . 52
5.2.1 Model Simulation . . . 52
5.2.2 FCFS Model . . . 53
5.2.3 Evaluation . . . 53
5.3 Model Efficacy with Threshold Change . . . 54
5.3.1 Model Simulation . . . 55
5.3.2 FCFS model . . . 55

5.3.3 Evaluation 56
5.4 Efficacy Test in Busiest Days 56

6 Results 57
6.1 Models Comparison 57
6.2 Feasibility Test 58
6.2.1 C40 Scenario 58
6.2.2 C100 Scenario 60
6.3 Efficacy without Threshold Change Test 61
6.3.1 C40 Scenario 61
6.3.2 C100 Scenario 64
6.4 Efficacy with Threshold Change Test 67
6.4.1 C40 Scenario 67
6.4.2 C100 Scenario 70
6.5 Efficacy Test in Busiest Days 73
6.5.1 C40 Scenario 73
6.5.2 C100 Scenario 75

7 Conclusion and Future Work 80
7.1 Conclusion 80
7.2 Future Work 81

Bibliography 82

1 Introduction

In this chapter, we discuss the motivation, context and objectives of this work. Besides, we present a literature review on the subject and point out the contributions of this undergraduate thesis. Lastly, we provide a description of the organization of the remaining chapters.

1.1 Motivation

In recent years, reflecting the growing global connectivity and economic development, the demand for air travel has increased significantly and is projected to continue to grow. According to the International Air Transport Association (IATA), the global number of air passengers is expected to reach 8.2 billion by 2037, nearly doubling the 4.1 billion passengers recorded in 2017. Also, as noted in Eurocontrol's Report of European Aviation (2040) — Challenges of Growth, this growth in air traffic is predicted to exacerbate airborne delays. By 2040, the number of passengers each day that experiences flights delays of 1-2 hours is expected to increase from 50,000 to 470,000 (EUROCONTROL, 2018).

This surge in air traffic, coupled with the anticipated rise in delays, underscores the critical need for advanced air traffic management (ATM) techniques. These techniques are essential to handle the growing volume of flights, ensuring that efficiency and safety are maintained, and mitigating the impact of increased delays.

Improving ATM not only enhances operational efficiency but also could have significant environmental benefits. According to IATA, aviation is responsible for 2% of global CO2 emissions, and this figure is expected to rise to 3% by 2050. The aviation industry's contribution to pollution includes not only CO2 but also other harmful pollutants, which have adverse effects on climate change and air quality. Efficient ATM can reduce fuel consumption and, consequently, emissions by minimizing unnecessary holding patterns, optimizing flight paths, and improving overall operational efficiency. This reduction in emissions is crucial for achieving sustainability goals and mitigating the environmental impact of the aviation industry.

To address these challenges, tools such as Arrival Manager (AMAN) systems have been developed to assist air traffic controllers (ATCOs) with optimizing arrival sequences at airports. AMAN systems, as described by Skybrary (Skybrary, 2024), provide automated sequencing support by continuously calculating arrival sequences and times for incoming flights, considering factors such as runway spacing and landing rates. By regulating the flow of traffic into busy airport zones, AMAN systems help manage airport capacity more effectively, contributing to a more efficient and predictable arrival process that reduces low-level holding and minimizes tactical interventions by ATCOs. These improvements also yield environmental benefits by lowering fuel consumption, noise, and emissions.

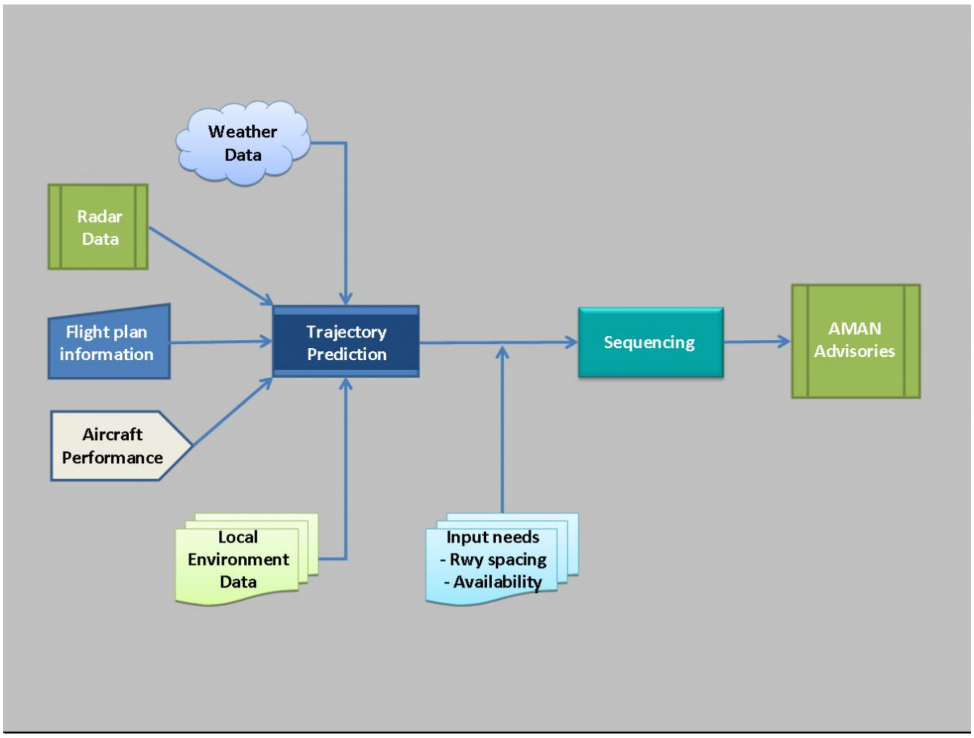

FIGURE 1.1 – Overview of AMAN System Data Flow (Skybrary, 2024).

Figure 1.1 provides an overview of the data flow in an AMAN system, which integrates inputs such as radar data, flight plans, weather data, and aircraft performance characteristics to predict trajectories. The sequencing module, highlighted in the figure, uses this information to optimize the order and timing of arriving aircraft, producing AMAN advisories to guide ATCOs.

The Sequencing component within AMAN is particularly relevant to this study, as it can be enhanced using Operational Research (OR) techniques. OR provides systematic methods for decision-making in complex real-life problems by applying mathematical models, statistical analyses, and optimization techniques. A specific branch of OR is Mixed-Integer Programming (MIP), a mathematical approach used to find the best possible solution for problems with both continuous and discrete variables. MIP is particularly well-suited when we are looking for solutions that adhere to operational constraints while optimizing the desired outcomes.

In this context, the Airspace Control Institute (ICEA), the Brazilian agency responsible for, among other tasks, air traffic control, faces the challenge of optimizing aircraft landing sequences, particularly at airports that lack tools to assist in this decision-making process — challenge that can be addressed by MIP model. This is the case at Guarulhos, São Paulo, International Airport, the busiest in the country. The necessity for enhanced sequencing solutions at such high-traffic hubs is imperative to manage the increased flow of aircraft efficiently and to reduce potential delays that could impact the national and international flight schedules.

1.2 Contextualization

According to (SILVA *et al.*, 2023), the increasing volume of flights and passengers has made airport runways one of the primary bottlenecks in ATM systems, and a critical factor in determining airport capacity. Due to economic and environmental constraints, expanding airport infrastructure cannot keep pace with the rapid growth of air traffic. Therefore, optimizing the use of existing infrastructure is essential to handle this growth effectively.

One of the primary strategies to enhance runway capacity is to optimize the sequencing of aircraft landings at airports. This challenge, known in academic literature as the Aircraft Landing Problem (ALP), involves assigning available runways for incoming aircraft and allocating a scheduled landing time for each (IKLI *et al.*, 2021). We can consider one or more runways. The goal is to optimize these landing times by minimizing the costs associated with earliness and lateness. The solution must consider operational constraints, such as the allowed time window, defined by an earliest and latest times possible for each aircraft to land.

Another important constraint in the ALP is the minimum separation time between consecutive landings. According to (FAHLE *et al.*, 2003), heavier and larger aircraft, such as the Boeing 747, generate stronger air turbulence (wake vortices), and aircraft must maintain a safe distance to avoid losing aerodynamic stability. Therefore, after a Boeing 747 lands, the following aircraft must wait a certain amount of time before landing to ensure safety. This separation time is determined by the International Civil Aviation Organization (ICAO) and varies according to the aircraft's weight category.

Several studies have successfully modeled the ALP using MIP and have achieved promising results. For example, (BEASLEY *et al.*, 2000) developed a MIP model to optimize aircraft landing sequences by minimizing delays and ensuring compliance with operational constraints, demonstrating the model's capability to handle complex scheduling tasks. Similarly, (BALAKRISHNAN; CHANDRAN, 2010) applied MIP to reduce taxiing times and improve runway throughput by optimizing aircraft sequencing and runway assignments. These studies highlight the versatility and effectiveness of MIP in enhancing airport operations, validating its applicability to the ALP in addressing the challenges of increasing air traffic and limited infrastructure.

As illustrated in Figure 1.1, AMAN systems can incorporate MIP techniques to optimize the Sequencing component, addressing the ALP in a way that enhances both capacity and efficiency. The ALP is considered an NP-hard problem (PRAKASH *et al.*, 2018), meaning that it is computationally intractable to solve optimally in polynomial time. As a result, for considering larger numbers of aircraft, some researchers have turned to heuristic and meta-heuristic algorithms to find near-optimal solutions within a reasonable time frame. Despite these complexities, MIP methods continue to effectively manage problems of realistic scales.

1.3 Objective

This study aims to develop a comprehensive model based on MIP to optimize aircraft sequencing at airports, assisting ICEA in gaining a deeper understanding of how AMAN systems work and identifying ways to improve the efficiency of air traffic management. To achieve this goal, we will address the following specific objectives:

1. Develop an initial MIP model for the ALP, incorporating constraints specified by ICEA.
2. Compare the initial model with a consolidated model from the literature using academic test data.
3. Enhance the initial model based on insights gained from the comparative analysis.
4. Assess the improved model's ability to generate timely solutions in scenarios involving high traffic volumes, using historical data from Guarulhos Airport.
5. Validate the improved model using historical data from Guarulhos Airport to demonstrate its effectiveness in optimizing aircraft sequencing and reducing delays.

1.4 Literature Review

The most cited MIP approach to the ALP was presented by (BEASLEY *et al.*, 2000). They propose the model for a single runway and after expand it to multiple runways. In their formulation, they take into account the minimal separation time between aircraft, enforced by wake vortex (VW) categories, as well as time windows constraints, and additional constraints that strengthen the linear programming relaxations. Their objective function is to minimize the total deviation from the target landing time, considering different costs for earliness and lateness. They also propose a Upper Bound heuristic to the problem. Finally, they solve their model using CPLEX and the proposed heuristic for a increasing number of runways in problems from the OR-library (BEASLEY, 1990), involving up to 50 aircraft and 4 runways.

Building upon Beasley's foundational model, (BRISKORN; STOLLETZ, 2014) adapted it to include objective functions that depend on aircraft class. They incorporated the Earliest Landing Window rule and achieved better computational times using CPLEX. (GHONIEM; FARHADI, 2015) further adapted this model to also encompass aircraft takeoffs, enhancing it with valid inequalities to tackle the complexities introduced by adding multiple runways and aircraft. Their empirical tests indicated that while valid inequalities and pre-processing could handle modest numbers of aircraft and runways, they were insufficient for larger scales. Consequently, they proposed a set-partitioning model solved through a column-generation approach, enabling the management of larger instances within reasonable computation times.

(FAYE, 2015) used a time-discretization approach on the same model, which presumed integer-valued problem parameters and thus also yielded integer-valued solutions. By discrediting the planning horizon into time slots, the approach limited possible landing scenarios, which simplified the problem into a manageable 0-1 linear problem solved using a dynamic constraints generation algorithm.

In parallel, (HANCERLIOGULLARI *et al.*, 2013) proposed a novel MIP formulation inspired by job-shop scheduling, which treated multiple runways as parallel machines, assuming independence in terms of separation requirements. This model also aimed at balancing traffic across available runways by imposing upper and lower bounds on the number of aircraft per runway, though it resulted in large computational times for optimal solutions.

Apart from MIP approaches, researchers have explored several alternative methodologies. Heuristic, meta-heuristic and reinforcement learning techniques have become increasingly prominent in solving the complex ALP, offering robust alternatives to traditional optimization methods. Notable studies leveraging Genetic Algorithms, such as those by (STEVENS, 1995) and (BEASLEY *et al.*, 2001), have demonstrated the potential of GAs in efficiently navigating the large solution spaces typical of ALP, resulting in high-quality solutions. Similarly, Ant Colony Optimization has been applied effectively in this domain by (BENCHEIKH *et al.*, 2009), showcasing the utility of biologically-inspired algorithms in optimizing aircraft landing sequences. Local Search strategies, explored by (SOOMER; FRANX, 2008), have proven valuable for refining solutions and enhancing algorithmic efficiency, particularly when integrated into larger heuristic frameworks. Additionally, (SOARES *et al.*, 2015) addressed the problem of scheduling aircraft take-offs on a single runway using reinforcement learning. By modeling the problem as a Markov Decision Process and applying Q-learning, they aimed to minimize delays while adhering to time windows. Their reinforcement learning approach performed comparably to human controllers in normal conditions and outperformed them under disturbances, demonstrating its potential for real-time optimization.

Finally, (VERESNIKOV *et al.*, 2019a; VERESNIKOV *et al.*, 2019b) and (IKLI *et al.*, 2021) provide extensive reviews of these methods, showcasing a broad spectrum of approaches and techniques developed over the years to solve various instances of the ALP, highlighting the continuous evolution and adaptation of optimization methods in air traffic management.

1.5 Contributions

The main contribution of this work is to propose a MIP model for optimizing aircraft sequencing in the context of the ALP, specifically tailored to meet the operational constraints required by ICEA. This model is designed to assist in understanding and enhancing the efficiency of AMAN systems by focusing on the sequencing module. By addressing this part of the system, the study supports ICEA in developing insights into AMAN functionality and potential improvements in high-traffic scenarios.

This work also contributes to the limited body of research on AMAN implementation in Brazilian air traffic management, providing a practical case study that highlights the model's ability to reduce delays and improve airport capacity management. The model was tested and compared against real operational data from Guarulhos International Airport, providing a valuable benchmark that demonstrates its practical applicability and effectiveness compared to current practices.

Furthermore, this study establishes a foundation for future research efforts aimed at building a comprehensive AMAN system. While the sequencing module here is enhanced through OR techniques, other components of the system may leverage different approaches, such as artificial intelligence. Future works can expand on this model, integrating various methodologies to develop a full AMAN system, aligning with ICEA's mission to advance air traffic management solutions in Brazil and support sustainable aviation objectives.

1.6 Outline of the Work

We organize the remaining chapters as follows:

- Chapter 2 cover integer mixed-integer programming theoretical background;
- Chapter 3 explains deeply the ASP and present the classic and the developed model for the problem;
- Chapter 4 details the methodology, including comparison methods, data acquisition, and an overview of the testing approach;
- Chapter 5 describes in detail the tests performed and the methods used to evaluate the model's performance;
- Chapter 6 shows the achieved results;
- Chapter 7 presents conclusions and suggests future work.

2 Theoretical Background

This section delves into the theoretical foundations of Mixed-Integer Programming within operational research, focusing on its structure, complexity, and solution methods. MIP combines aspects of both linear programming and integer programming, allowing for the inclusion of both continuous and integer decision variables, making it highly applicable for optimization problems in logistics, scheduling, finance, and beyond. A cornerstone of MIP solution techniques is the Simplex method, widely used in linear programming due to its efficient navigation of extreme points in a solution space. Here, we provide an overview of the core concepts in MIP, the role of the Simplex method, and the mechanisms for ensuring integer constraints, particularly through methods like branch-and-bound.

2.1 MIP: Formulation and Applications

Mixed-Integer Programming is a specialized optimization model that represents a linear objective function subject to constraints, where some or all of the decision variables are restricted to integer values. The general form of a MIP problem is expressed as:

$$\text{Maximize (or Minimize)} \quad f(x) = c^T x \tag{2.1}$$

$$\text{Subject to} \quad Ax \leq b, \quad x \in \mathbb{Z}^p \times \mathbb{R}^{n-p} \tag{2.2}$$

where x represents the vector of decision variables, partitioned into integer ($x \in \mathbb{Z}^p$) and continuous components ($x \in \mathbb{R}^{n-p}$), with coefficients c, b, and A defining the constraints and objective function. The inclusion of integer constraints broadens the applicability of the model, enabling it to capture decisions that require discrete choices, such as the number of items produced, binary decisions for project selection, routing constraints in transportation, and even sequencing tasks.

2.2 Complexity and Challenges of MIP

MIP is inherently NP-hard due to the discrete nature of integer variables. Unlike linear programming, where feasible regions form a continuous, convex space, the feasible solution space in MIP is fragmented by integer constraints, which introduces computational challenges. As a result, finding an optimal solution can be highly complex, especially for large-scale problems. To address these challenges, solution techniques must account for the combinatorial explosion in possible integer solutions, often using iterative methods and heuristics to manage the computational demands effectively.

2.3 The Fundamental Theorem of Linear Programming

The fundamental theorem of linear programming states that, in a linear programming problem with a bounded and non-empty feasible region, the optimal solution will be found at one of the vertices (or extreme points) of this feasible region, often represented as a polytope (LUENBERGER; YE, 2008). This theorem is essential because it allows optimization algorithms, such as the Simplex method, to focus only on the vertices of the feasible region instead of searching throughout. This focus on extreme points reduces computational time and makes the Simplex method one of the most effective approaches for solving linear programming problems.

2.4 The Simplex Method: Efficient Traversal of Vertices

The Simplex method is a widely utilized algorithm in linear programming, celebrated for its efficiency in locating optimal solutions by moving along the vertices, or extreme points, of a polytope that defines the feasible region (BAZARAA *et al.*, 2005). At each step, the Simplex method traverses the edges of this convex polytope, moving from one vertex to another in a direction that optimizes the objective function. This traversal continues until an optimal vertex is identified, where no further improvement is possible.

In the context of MIP, the Simplex method serves an essential role in the preliminary step of solving the linear relaxation of the integer-constrained problem. The relaxation involves solving the problem without integer constraints, allowing variables to take on continuous values. This step generates a baseline solution that informs further search within the MIP framework. By providing bounds and initial feasible points, the Simplex method sets the stage for techniques that enforce integer constraints, such as branch-and-bound and branch-and-cut methods (ARENALES *et al.*, 2007).

2.5 Branch-and-Bound and Branch-and-Cut

The branch-and-bound algorithm is a fundamental technique in MIP for ensuring integer feasibility in solutions. This approach begins with the linear relaxation solution (often obtained through the Simplex method) and iteratively partitions the solution space by creating subproblem, or “branches”. Each branch represents a subset of the feasible region, with additional constraints introduced to enforce integer solutions. For each subproblem, bounds are calculated using the Simplex method, and branches that cannot yield a better solution than the current best are “pruned” from the search space, effectively narrowing down the solution space.

Branch-and-cut is an enhancement of the branch-and-bound method that incorporates additional linear constraints, or “cuts”, to further restrict the feasible region and exclude fractional solutions without exploring unnecessary branches. By integrating cutting planes with the branching process, branch-and-cut refines the feasible region more rapidly, improving computational efficiency while ensuring integer solutions.

Both branch-and-bound and branch-and-cut rely on the Simplex method’s efficiency for solving each relaxed problem, making it integral to these algorithms’ performance and effectiveness in MIP (ARENALES *et al.*, 2007).

3 Aircraft Landing Problem

When an aircraft approaches an airport, it requires the air traffic control control to allocate a landing time and designate an appropriate runway. These assignments are governed by specific constraints, detailed in the ensuing sections.

3.1 Main Constraints

The ALP hinges critically on two main constraints: the prescribed time window for each aircraft and the required minimum separation between landings.

3.1.1 Time Window Constraint

Each airplane has a time window in which it can land. This time window is defined by the earliest and latest landing times. The earliest time represents the situating of the aircraft flying at its maximum speed. Conversely, the latest permissible time represents the situating of the aircraft flying at its most fuel-efficient speed while maximizing holding time.

Additionally, each plane has a target landing time, which is the ideal landing moment assuming no deviations from its preferred speed and trajectory. Deviations from this target, whether earlier or later, incur specific costs.

3.1.2 Minimum Separation Constraint

Air traffic control must ensure a safe separation between aircraft. An aircraft generates Wake Vortex turbulence, which can affect subsequent aircraft during landing. Therefore, a minimum safe separation must be established to ensure the stability of the aircraft. For this purpose, the International Civil Aviation Organization (ICAO) classifies aircraft into four categories based on their maximum takeoff mass. The separation required between landings thus depends on the categories of both the leading and the following aircraft.

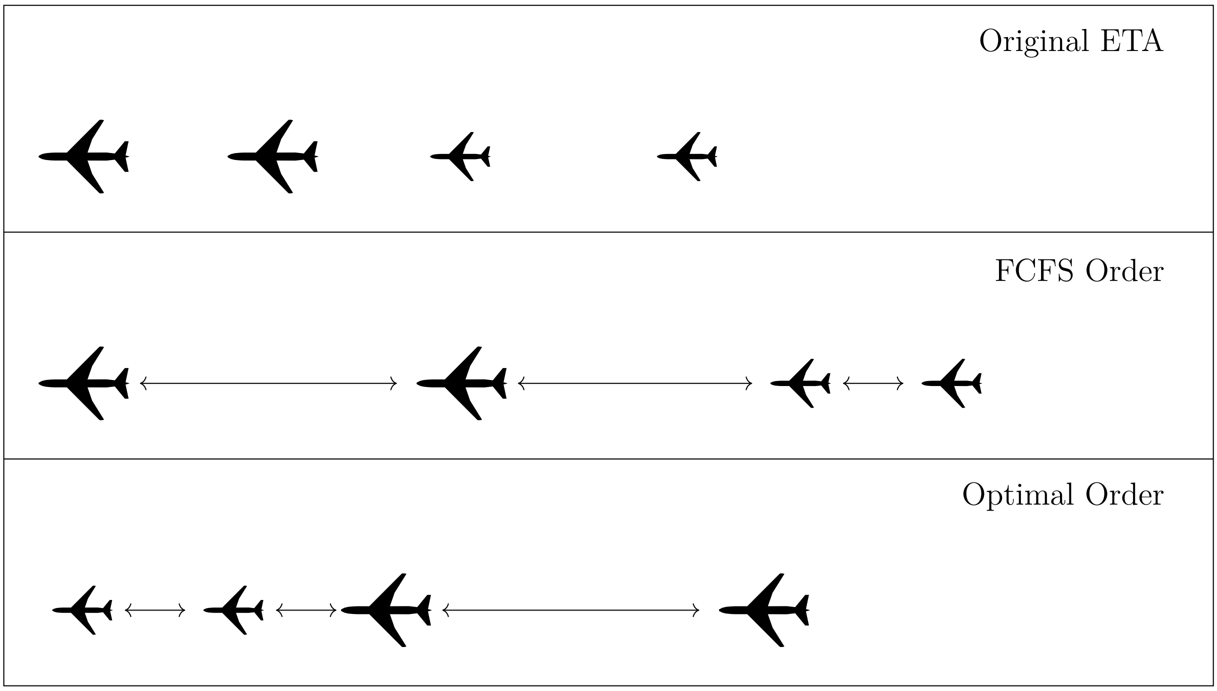

FIGURE 3.1 – Comparison between the FCFS and the optimal order.

A commonly employed sequencing strategy is First-Come-First-Served (FCFS), which allocates landing times based on the order of aircraft arrival, considering the Estimated Time of Arrival (ETA). Under this strategy, the first aircraft to arrive is given the earliest available landing slot, continuing in sequence. This method is straightforward, minimizes controller workload, and maintains fairness among incoming flights, as no aircraft is delayed beyond the minimum required separation. However, at busy airports, the rigidity of minimum separation distances means that FCFS may not always yield the most efficient sequence in terms of reducing overall delays or maximizing runway throughput.

Figure 3.1 depicts the differences between FCFS and optimal sequencing strategies. The top panel shows the original aircraft sequencing with landing times set by each aircraft's ETA. The middle panel shows FCFS sequencing, which adheres to the necessary separation constraints. The bottom panel displays optimal sequencing, aimed at minimizing total aircraft delays. In this example, considerations for individual aircraft's landing time windows were omitted.

We can observe that due to the greater minimum separation required when a larger aircraft is the lead aircraft, FCFS is not always able to provide the most efficient sequencing. This happens specially in congested airports scenarios, where the difference between airplane's ETA is lower.

3.2 Additional Constraints

Beyond the main constraints, there are other considerations that may be factored into the ALP, such as the prioritization of certain aircraft, the management of emergency aircraft and accounting for threshold changes. These considerations, particularly relevant in Brazilian airspace, can significantly enhance the efficiency of aircraft sequencing in specific scenarios.

3.2.1 Priority Aircraft

Priority aircraft include those designated for expedited handling due to factors such as diplomatic importance, critical cargo, or scheduling requirements. The optimization model used for ALP should, therefore, prioritize minimizing the landing delays for these aircraft. By doing so, the model ensures that priority aircraft meet their critical timelines, thereby reducing potential disruptions in the broader network and maintaining high service levels for important flights.

3.2.2 Emergency Aircraft

Emergency aircraft are those facing urgent conditions that pose immediate risks to passenger and crew safety or to the aircraft's integrity, such as medical emergencies or significant mechanical failures. It is imperative that these aircraft are given the highest priority for landing.

To prevent any incidents that could render a runway unavailable — such as a crash or a runway blockage due to a disabled aircraft — emergency aircraft are mandated to land first on any available runway. However, in situations where the number of emergency aircraft exceeds the available runways, not all emergency aircraft can land first. This directive ensures that no other aircraft are permitted to land until the situation is completely resolved and the runway is officially clear.

This precaution is crucial to maintaining runway readiness solely for emergency landings, ensuring that these critical situations are handled without additional risks or disruptions.

3.2.3 Threshold change

A critical consideration in the ALP is the potential for runway threshold changes, which may occur in response to factors such as wind direction and other meteorological conditions. During landing operations, the runway threshold (the designated beginning of the landing runway) can be adjusted to ensure safety and efficiency under varying weather conditions. Although a predictive system exists that can provide information on threshold changes with a 15-minute notice specifically for Guarulhos International Airport (ICEA, 2023), aircraft are currently informed of these changes only immediately prior to landing. This short-notice adjustment can lead to increased delays, as both pilots and air traffic controllers must quickly adapt to the new configuration.

Incorporating threshold change information into the optimization model is essential for minimizing delays associated with these adjustments. By allowing the model to receive information regarding if and when a threshold change will occur, as well as the estimated landing times for both possible thresholds, the optimization process can proactively sequence aircraft to accommodate these changes. This advance consideration enables the model to reduce disruptions caused by sudden threshold reassignments, ensuring a smoother flow of landings even in dynamically shifting conditions.

With this enhanced capability, the model can prioritize aircraft sequencing to account for upcoming threshold adjustments, thereby mitigating potential delays and improving overall operational efficiency. By optimizing the landing sequence in anticipation of threshold changes, the model not only improves adherence to planned arrival times but also enhances the resilience of airport operations under varying weather conditions. This approach supports a more reliable and adaptable air traffic management system, particularly in high-traffic environments where minor delays can have significant cascading effects on the airport's schedule and capacity.

3.3 Classic ALP Model

In this section, we introduce the classic model based on MIP for the ALP. This model is based on the work presented in (BEASLEY *et al.*, 2000).

3.3.1 Parameters

In the model, we consider the following defined parameters:

N the set of aircraft $N = \{1, 2, \ldots, n\}$;

R the set of runways $R = \{1, 2, \ldots, n_r\}$;

T_i the target time for each aircraft $i \in N$ to land;

E_i the earliest time that aircraft $i \in N$ can land;

L_i the latest time that aircraft $i \in N$ can land;

A_i the cost of anticipation for aircraft $i \in N$;

B_i the cost of delay for aircraft $i \in N$;

S_{ij} the minimum separation time between aircraft $i \in N$ and aircraft $j \in N$ on the same runway, $i \neq j$;

s_{ij} the minimum separation time between aircraft $i \in N$ and aircraft $j \in N$ on different runway, $i \neq j$;

3.3.2 Variables

Variables in the model are defined as follows.

t_i the landing time for aircraft $i \in N$;

a_i the delay time for aircraft $i \in N$;

b_i the anticipation time for aircraft $i \in N$;

$$x_{ij} = \begin{cases} 1, & \text{if aircraft } i \text{ lands before aircraft } j\text{, with } i, j \in N \text{ and } i \neq j \\ 0, & \text{otherwise} \end{cases}$$

$$z_{ij} = \begin{cases} 1, & \text{if aircraft } i \text{ and } j \text{ land on the same runway, with } i, j \in N \text{ and } i \neq j \\ 0, & \text{otherwise} \end{cases}$$

$$y_{ir} = \begin{cases} 1, & \text{if aircraft } i \text{ lands on runway } r\text{, with } i \in N \text{ and } r \in R \\ 0, & \text{otherwise} \end{cases}$$

3.3.3 Constraints

The first set of constraints is defined as:

$$E_i \leq t_i \leq L_i, \qquad \forall i \in N, \tag{3.1}$$

which ensures that the landing time for each aircraft i is within its defined time window. Additionally, for each pair of aircraft i and j, we have:

$$x_{ij} + x_{ji} = 1, \qquad \forall i, j \in N,\ j > i. \tag{3.2}$$

This ensures that aircraft i must land either before or after aircraft j.

Furthermore, we have:

$$\sum_{r \in R} y_{ir} = 1, \qquad \forall i \in N, \tag{3.3}$$

ensuring that each aircraft i lands on only one runway.

To adjust the binary variable z_{ij}, we must ensure symmetry such that if aircraft i lands on the same runway as aircraft j, then aircraft j lands on the same runway as aircraft i. This is guaranteed by the set of constraints:

$$z_{ij} = z_{ji}, \qquad \forall i, j \in N,\ j \geq i. \tag{3.4}$$

Moreover, if there is a runway r where both aircraft i and j land, i.e., $y_{ir} = y_{jr} = 1$, then $z_{ij} = 1$. If $z_{ij} = 0$, then i and j cannot land on the same runway, i.e. y_{ir} and y_{jr} cannot both be 1. This condition is guaranteed by:

$$z_{ij} \geq y_{ir} + y_{jr} - 1, \qquad \forall i, j \in N,\ j \geq i,\ r \in R. \tag{3.5}$$

To ensure minimum separation between aircraft, we have the constraints:

$$t_j \geq t_i + S_{ij} z_{ij} + s_{ij}(1 - z_{ij}) - M(1 - x_{ij}), \qquad \forall i, j \in N,\ i \neq j, \tag{3.6}$$

where M is a sufficiently large positive constant. We consider four cases:

1. Aircraft i lands before aircraft j ($x_{ij} = 1$) on the same runway ($z_{ij} = 1$). Equation (3.6) becomes:

$$t_i \geq t_j + S_{ij}, \tag{3.7}$$

ensuring the appropriate minimum separation.

2. Aircraft i lands before aircraft j ($x_{ij} = 1$) on different runways ($z_{ij} = 0$). Equation (3.6) becomes:

$$t_i \geq t_j + s_{ij}, \tag{3.8}$$

ensuring the appropriate minimum separation.

3. Aircraft i lands after aircraft j ($x_{ij} = 0$) on the same runway ($z_{ij} = 1$). Equation (3.6) becomes:

$$t_i \geq t_j + S_{ij} - M, \tag{3.9}$$

in this case, since M is a sufficiently large constant, t_j is effectively unrestricted by a negative bound, which deactivates the constraint.

4. Aircraft i lands after aircraft j ($x_{ij} = 0$) on different runways ($z_{ij} = 0$). The Equation becomes:

$$t_i \geq t_j + s_{ij} - M, \tag{3.10}$$

in this case, as in the previous one, the constraint is effectively deactivated.

To relate the variables t_i with the delay time a_i or the advancement time b_i for each aircraft i, we use the constraints:

$$t_i = T_i + a_i - b_i, \qquad \forall i \in N. \tag{3.11}$$

Finally, we define intervals for the anticipation and delay time variables:

$$a_i \geq t_i - T_i, \qquad \forall i \in N, \tag{3.12}$$

$$b_i \geq T_i - t_i, \qquad \forall i \in N, \tag{3.13}$$

$$0 \leq a_i \leq L_i - T_i, \qquad \forall i \in N, \tag{3.14}$$

$$0 \leq b_i \leq T_i - E_i, \qquad \forall i \in N. \tag{3.15}$$

Equations (3.12) and (3.14) ensure that a_i is at least as big as zero and the difference between the landing and target times, and at most the difference between the latest allowed and target times. Equations (3.13) and (3.15) ensure are similar, but for b_i.

3.3.4 Objective Function

The objective function is defined to minimize the total cost of anticipation and delay for all aircraft:

$$\min \sum_{i \in N} (A_i a_i + B_i b_i). \tag{3.16}$$

3.4 Implemented Model

In this section, we present an independently developed model, prior to our exploration of the classic model detailed in Section 3.3. It maintains a structural similarity, including several constraints that echo those found in the classic model. However, it introduces variations in the decision variables and integrates additional constraints designed to meet specific operational demands.

A key addition is a restriction preventing the first plane predicted to land from advancing beyond its ETA, ensuring minimum separation and reducing the risk of safety issues with aircraft that may have just landed. The model also emphasizes the prioritization of emergency and high-priority aircraft, aligning it with real-world air traffic control requirements and safety protocols.

By integrating these elements, the model provides a framework that not only reflects the theoretical structure of the classic approach but also addresses practical demands for efficient and safe air traffic management.

3.4.1 Main Differences

The primary difference lies in the definition of the binary decision variable x_{ij}. In our definition this variable has been given an additional dimension, with respect to the landing runway. Futhermore, instead of being set to 1 if aircraft i lands before aircraft j, x_{ijr} is set to 1 only if aircraft i is the aircraft that immediately precedes aircraft j in the landing sequence of runway r. This precise definition enables the model to operate without the variable z_{ij} and y_{ir}, present in the classic model. Therefore:

$$x_{ijr} = \begin{cases} 1, & \text{if aircraft } i \text{ lands immediately before aircraft } j \text{ in runway } r, \\ & \text{with } i, j \in N,\ r \in R \text{ and } i \neq j \\ 0, & \text{otherwise.} \end{cases}$$

To accommodate this setup, the model incorporates a fictitious aircraft concept, defined as aircraft 0, which is assumed to immediately precede the first landing aircraft and immediately succeed the last. This means that if aircraft f is the first to land on runway r, then $x_{0fr} = 1$, and if aircraft l is the last to land on runway r, then $x_{l0r} = 1$. This requires the binary matrix x to be dimensioned at $n + 1 \times n + 1 \times r$.

In order to facilitate notation, consider the new set $N' = N \cup \{0\}$, representing the set of all aircraft, including the fictitious aircraft.

Another key difference is that in this model we implemented the emergency and high-priority aircraft related constraints discussed in Section 2.2. For this, we will consider the new parameters:

P_i a binary variable that indicates if aircraft $i \in N$ is a priority aircraft;

U_i a binary variable that indicates if aircraft $i \in N$ is an emergency aircraft;

The final difference is that our approach does not consider minimal separation for aircraft landing on different runways, reflecting the assumption that aircraft on separate runways do not interfere with each other's operations.

3.4.2 Constraints

Given the unique definition of the decision variable x_{ijr}, and the absence of variables z_{ij} and y_{ir}, our model incorporates different constraints to accommodate this setup.

For every available runway r, the fictitious aircraft must immediately precede and also immediately follow some aircraft — even if it means this fictitious aircraft is preceding or following itself. This setup is formalized by the following constraints:

$$\sum_{j \in N'} x_{0jr} = \sum_{i \in N'} x_{i0r} = 1, \qquad \forall r \in R. \tag{3.17}$$

Additionally, each non-fictitious aircraft must have exactly one immediate successor and one immediate predecessor across all landing runways. This ensures each aircraft is uniquely positioned in the landing sequence:

$$\sum_{\substack{j \in N' \\ r \in R}} x_{ijr} = \sum_{\substack{j \in N' \\ r \in R}} x_{jir} = 1, \qquad \forall i \in N,\ i \neq j. \tag{3.18}$$

Furthermore, it is necessary to ensure that the immediate predecessor and successor of each aircraft are on the same runway:

$$\sum_{j \in N'} x_{ijr} = \sum_{j \in N'} x_{jir}, \qquad \forall i \in N',\ i \neq j,\ \forall r \in R. \tag{3.19}$$

Since we do not consider minimum separation between aircraft landing on different runways (s_{ij}), and the variable z_{ij} is not present, the minimum separation constraints are simplified to:

$$t_j \geq t_i + S_{ij} - M(1 - x_{ijr}), \qquad \forall i, j \in N,\ i \neq j,\ \forall r \in R. \tag{3.20}$$

The other constraints are equivalent to Equations (3.1) and (3.11) to (3.15) of the classic model.

3.4.3 New Constraints

3.4.3.1 Priority and Emergency Aircraft

In addressing emergency flights, it is critical to ensure that their landing times are prioritized to be as early as possible:

$$t_i \geq t_j - M(1 - U_j + U_i) - M(2 - \sum_{k \in N'} x_{ikr} - \sum_{k \in N'} x_{jkr}) \qquad (3.21)$$

$$\forall i, j \in N,\ i \neq j,\ \forall r \in R.$$

To understand this constraint, consider that if two aircraft, i and j, both land on the same runway r, then both have immediate successors on that runway, which implies that $(\sum_{k \in N'} x_{ikr} + \sum_{k \in N'} x_{jkr} = 2)$. Under this condition, we analyze four distinct cases:

1. Aircraft j is not an emergency flight ($U_j = 0$). Equation (3.21) becomes:

$$t_i \geq t_j - M(1 + U_i) - M(2 - \sum_{k \in N'} x_{ikr} - \sum_{k \in N'} x_{jkr}), \qquad (3.22)$$

   in this case, since M is a large constant, for every value of U_i the time t_i effectively becomes greater than or equal to a very large negative number, and the constraint becomes deactivated.

2. Both aircraft i and j are emergency flights ($U_i = U_j = 1$). Equation (3.21) becomes:

$$t_i \geq t_j - M - M(2 - \sum_{k \in N'} x_{ikr} - \sum_{k \in N'} x_{jkr}), \qquad (3.23)$$

   in this scenario, the constraint also becomes deactivated due to the large value of M.

3. Aircraft j is an emergency flight ($U_j = 1$), aircraft i is not ($U_i = 0$), and they do not both land on the same runway r ($\sum_{k \in N'} x_{ikr} + \sum_{k \in N'} x_{jkr} < 2$). The Equation becomes:

$$t_i \geq t_j - M, \qquad (3.24)$$

   again, the constraint is effectively deactivated.

4. Aircraft j is an emergency flight ($U_j = 1$), aircraft i is not ($U_i = 0$), and both aircraft land on the same runway r ($\sum_{k\in N'} x_{ikr} + \sum_{k\in N'} x_{jkr} = 2$). The Equation simplifies to:

$$t_i \geq t_j, \tag{3.25}$$

this ensures that aircraft i lands after aircraft j, prioritizing the emergency landing

Finally, we need to ensure that emergency flights are the first to land on each runway unless another emergency flight has landed before. This is guaranteed by the following set of constraints:

$$\sum_{\substack{j\in N\\ r\in R}} x_{0jr}\, U_j \geq \min(n_r, \sum_{i\in N} U_i), \qquad \forall i \in N. \tag{3.26}$$

The left side of Equation (3.26) represents the number of all emergency flights that are the immediate successors of the fictitious flight on the available runways, i.e., the number of emergency flights that are the first to land on the runway. This must be at least equal to the lesser of the number of runways or the number of emergency flights.

3.4.3.2 Preventing advancement of the first aircraft

In order to prevent the first aircraft from advancing beyond its ETA, we introduce the new binary decision variable w_{ir}, which is set to 1 if aircraft i is the first to land on runway r:

$$w_{ir} = \begin{cases} 1, & \text{if aircraft } i \text{ is the first to land on runway } r, \\ & \text{with } i \in N \text{ and } r \in R, \\ 0, & \text{otherwise.} \end{cases} \tag{3.27}$$

Additionally, we introduce the following:

$$\sum_{i\in N} w_{ir} = 1, \qquad \forall r \in R, \tag{3.28}$$

ensuring that only one aircraft is the first to land on each runway.

Furthermore, to define as the first aircraft to land on each runway as the one with the least t_i, we have:

$$t_i - t_j \leq M(1 - w_{ir}) - M(2 - \sum_{k\in N'} x_{ikr} - \sum_{k\in N'} x_{jkr}) \tag{3.29}$$

$$\forall i, j \in N,\ i \neq j,\ \forall r \in R.$$

To understand this constraint, note that if two aircraft, i and j, both land on the same runway r, $(\sum_{k\in N'} x_{ikr} + \sum_{k\in N'} x_{jkr} = 2)$. Under this condition, we analyze three distinct cases:

1. Aircraft i and j do not both land on the same runway r $(\sum_{k\in N'} x_{ikr}+\sum_{k\in N'} x_{jkr} < 2)$. Equation 3.29 becomes:

$$t_i - t_j \leq M(1 - w_{ir}) - M, \tag{3.30}$$

   the constraint is effectively deactivated.

2. Aircraft i and j both land on the same runway r $(\sum_{k\in N'} x_{ikr} + \sum_{k\in N'} x_{jkr} = 2)$ and i is not the first of the sequence in r $(w_{ir} = 0)$. Equation 3.29 becomes:

$$t_i - t_j \leq M, \tag{3.31}$$

   the constraint also becomes deactivated.

3. Aircraft i and j both land on the same runway r $(\sum_{k\in N'} x_{ikr} + \sum_{k\in N'} x_{jkr} = 2)$ and i is the first of the sequence in r $(w_{ir} = 1)$. The Equation becomes:

$$t_i \leq t_j, \qquad \forall j \in N, \tag{3.32}$$

   in this case, the constraint ensures that aircraft i lands before all other aircraft on runway r.

Finally, we need to ensure that the first aircraft to land on each runway does not advance beyond its ETA. This is guaranteed by:

$$b_i \leq 1 - w_i + M(1 - w_i), \qquad \forall i \in N, \tag{3.33}$$

We have:

1. Aircraft i is the not the first to land on runway r $(w_{ir} = 0)$. Equation 3.33 becomes:

$$b_i \leq 1 + M, \tag{3.34}$$

   the constraint is effectively deactivated.

2. Aircraft i is the first to land on runway r $(w_{ir} = 1)$. Equation 3.33 becomes:

$$b_i \leq 0, \tag{3.35}$$

   which ensures that $b_i = 0$.

3.4.4 Objective Function

In this model, we prioritize the class of priority flights. Thus, the objective function is similar to that of Equation (3.16) but focuses on minimizing the costs for flights of the priority class:

$$\min \sum_{i \in N} (A_i a_i + B_i b_i)(1 + MP_i) \tag{3.36}$$

3.5 Model with Threshold Change

In addition to the primary model, we implemented an enhanced version that accounts for threshold changes. This model retains the core structure of the initial model but includes additional constraints to address runway threshold adjustments. These constraints enable the model to dynamically adapt landing sequences in response to anticipated threshold changes, thus optimizing the landing schedule in scenarios where runway configurations shift due to factors such as wind direction or other operational requirements.

By incorporating these adjustments, the model can minimize delays that might otherwise arise from last-minute threshold changes. The added constraints ensure that projected landing times are calculated for both current and anticipated threshold positions, allowing the model to prioritize aircraft sequencing accordingly. This approach enhances the resilience of airport operations, particularly in high-traffic environments, by reducing the impact of sudden changes in runway alignment.

To achieve this, we consider the following new parameters:

$T1_i$ the target time if aircraft $i \in N$ were to land at threshold 1;

$T2_i$ the target time if aircraft $i \in N$ were to land at threshold 2;

C the time at which the threshold change occurs.

Additionally, two new decision variables are introduced:

T_i the actual target time for aircraft $i \in N$;

$$c_t = \begin{cases} 1, & \text{if aircraft } i \text{ lands at threshold 1, with } i \in N, \\ 0, & \text{if aircraft } i \text{ lands at threshold 2, with } i \in N. \end{cases}$$

For constraints, all equations that originally included the parameter T now consider the decision variable T instead. In addition, we must ensure correct landing times for aircraft landing on each threshold. Specifically, we need to guarantee that if an aircraft is assigned to land at threshold 1, it completes its landing before the threshold change time C, and conversely, if it is assigned to threshold 2, its landing occurs after this change. This is enforced through the following constraint:

$$t_i \leq C + M\ c_i, \qquad \forall i \in N; \tag{3.37}$$

$$t_i \geq C - M\ (1 - c_i), \qquad \forall i \in N; \tag{3.38}$$

To understand this, consider two scenarios:

1. Aircraft i lands at threshold 1 ($c_i = 0$). Equations (3.37 e 3.38) become:

$$t_i \leq C, \tag{3.39}$$
$$t_i \geq M, \tag{3.40}$$

   ensuring that flight i lands before the threshold change.

2. Aircraft i lands at threshold 2 ($c_i = 1$). Equations (3.37 e 3.38) become:

$$t_i \leq M, \tag{3.41}$$
$$t_i \geq C, \tag{3.42}$$

   ensuring that flight i lands after the threshold change.

Finally, we must ensure that the actual target time T_i for each aircraft is correctly assigned. This is achieved through the following constraint:

$$T_i = c_i\ T1_i + (1 - c_i)\ T2_i, \qquad \forall i \in N. \tag{3.43}$$

4 Methodology

In this chapter, we detail the process for comparing the models introduced in the previous section. We also outline our approach to evaluating the model's performance across different traffic scenarios, utilizing real data from Guarulhos International Airport. Furthermore, we explain the methods of data acquisition and preparation, ensuring accurate and reliable inputs for analysis.

4.1 Comparison with the Classic Model

Both our model and the classical model, described in Section 2.1, were implemented using Julia 1.10.3 with the Gurobi 11.0.2 solver API. We subsequently compared these models using test data sourced from the OR-Library (BEASLEY, 1990), a resource commonly referenced in the literature. Our analysis accommodated scenarios involving up to 44 aircraft and 3 runways. It's important to note that the data did not account for flights classified by priority or emergency status, and there was no minimum separation enforced between aircraft landing on different runways ($s_{ij} = 0$), enabling a straightforward comparison between the two models.

Numerical tests were conducted on a computer equipped with an Intel Core i7-1260P processor and 16GB of RAM, operating under Ubuntu 22.04.

Following the comparison, as discussed in Section 6.1, we observed that the classic model demonstrated a certain advantage in performance. Consequently, all additional constraints specified in Sections 3.4.3 and 3.5, including those addressing priority and emergency handling, threshold changes, and the restriction preventing the first plane from advancing beyond its ETA, were implemented in the classic model. Moving forward, we will refer to this enhanced version of the classic model, which now includes our additional constraints, as the proposed model.

To evaluate the proposed model, we examined its optimization output, which includes the landing sequence for all aircraft, specific landing times, and required actions to maintain this sequence — whether through applying landing delays or advances. Figure 4.1

presents an example of the optimization output.

```
-------------------------------------------------------------------
flight        id  type            action    landing time   ETA
------ ---------  ----  ----------------  --------------  -----
     1    ITY674     3          delay 28             331    303
     2   GLO1527     2               ---             211    211
     3    DLH506     3               ---              49     49
     4    AMX014     3        advance 13             686    699
     5   TAM8113     3               ---             626    626
     6   GLO1609     2               ---             436    436
     7   TAM4555     2          delay 39             746    707

Runway 1: | 3 | 2 | 1 | 6 | 5 | 4 | 7 |
-------------------------------------------------------------------
```

FIGURE 4.1 – Example of optimization output.

Using this output, we conducted tests to assess the effectiveness of the proposed model with real data from Guarulhos International Airport. The testing process was organized into four stages, which will be explained in the following sections. Prior to testing, the real data had to be acquired and prepared, as described in the next section.

4.2 Data Acquisition and Preparation

The data used in this evaluation was provided by ICEA and comprised the following primary sources:

- **Radar Data**: This dataset contains real-time aircraft positions with geographical coordinates recorded at four-second intervals.
- **Air Traffic Movement Information Bank (BIMTRA) Table**: This comprehensive table logs flight information, including details such as aircraft identification, assigned runway, flight category (arrival or departure), landing or departure times, aircraft model, and performance indicators.
- **Meteorological Aerodrome Report (METAR) Table**: This table provides hourly meteorological reports for Guarulhos International Airport, detailing weather conditions such as visibility, wind speed, and cloud cover.

Specific days and periods were selected from the radar data to suit each test. Additionally, flights were considered from two distances relative to the airport: 40 and 100 nautical miles — standards set by the Department of Airspace Control (DECEA). This setup, using cylindrical boundaries with radii of 40 (C40) and 100 (C100) nautical miles

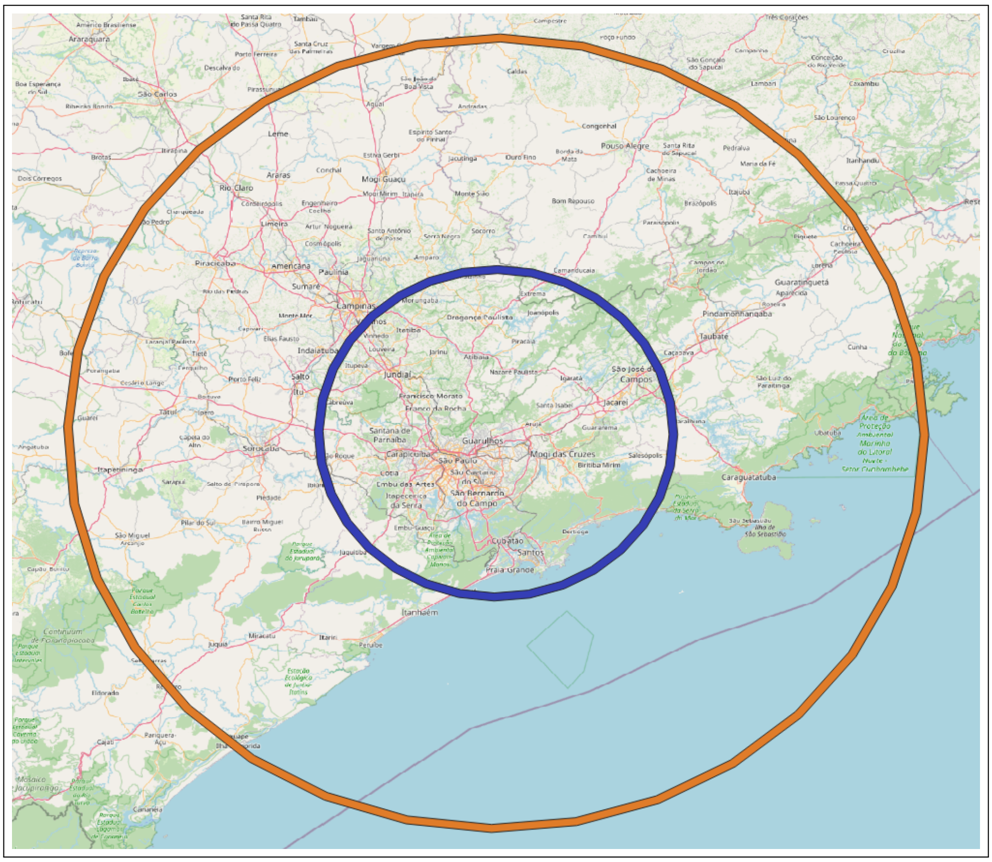

FIGURE 4.2 – Boundaries at 40 (inner circle) and 100 (outer circle) nautical miles centered on Guarulhos Airport.

centered on the airport, allowed for an assessment of the model's efficacy under varying traffic scenarios. Figure 4.2 presents an image of these boundaries around Guarulhos.

This boundary definition ensures that all relevant flights within these control zones are included in the sequence optimization.

With the filtered radar data, additional required information was obtained for each flight. The following sections explain the process of data acquisition for each parameter used in the model.

4.2.1 Set of Aircraft and Runways

The set of aircraft (N) varied depending on the number of flights present in the radar data during different time intervals. For each selected period, we created a set of active aircraft, with each aircraft represented by a unique identifier. The set of runways (R), however, remained fixed, as Guarulhos International Airport operates with only one active runway for landing sequences.

4.2.2 Target landing time

The target landing time is a crucial parameter in our optimization model, representing the ideal landing time for an aircraft under optimal conditions. In this study, we selected the unimpeded time as the target landing time for each aircraft. This decision was driven by the fact that airline-scheduled landing times are often conservative, incorporating buffer periods to account for potential delays. Consequently, scheduled times do not accurately reflect the optimal landing time under ideal conditions. Furthermore, there is no consistent or reliable method for predicting exact landing times based solely on operational data.

According to the aeronautical guidelines (DECEA, 2020b), the unimpeded time represents the time an aircraft would take to land from a specific distance if no additional sequencing delays or disruptions were present. This value is determined based on the aircraft type, runway in use, and the sector from which the aircraft enters the control area. The unimpeded time serves as a more realistic and reliable metric for modeling purposes, reflecting an ideal operational scenario.

The unimpeded time was estimated following a statistical analysis of historical flight data, as recommended by (DECEA, 2020b). Historical data from ICEA was categorized based on the following parameters:

- **Sector of entrance**: Calculated based on the aircraft's entry angle into the C40 boundary;
- **Runway of landing**: The actual runway used by the aircraft;
- **Aircraft category**: Classified as Light, Medium, Heavy, and Super, according to wake turbulence categories.

For each group, the unimpeded time was calculated as the 20th percentile of the landing times observed under similar conditions, ensuring that the estimated target time represents an ideal landing scenario. Pre-calculated unimpeded times were obtained for distances of 100 and 40 nautical miles from the airport. When target times for distances between these predefined points were required, interpolation was applied.

By employing unimpeded time as the target landing time, the model operates on a realistic approximation of optimal conditions, avoiding the biases introduced by conservative airline scheduling practices. This approach ensures that the aircraft sequencing model is grounded in data-driven, operationally meaningful metrics.

4.2.2.1 Sector of Entrance

The sector of entrance refers to the angle at which an aircraft enters the cylindrical boundary (C40 or C100) around the airport, measured from 0° to 360°, with 0° corresponding to north. This boundary is divided into six sectors, each covering 60 degrees:

- Sector 1: 0° to 60°
- Sector 2: 60° to 120°
- Sector 3: 120° to 180°
- Sector 4: 180° to 240°
- Sector 5: 240° to 300°
- Sector 6: 300° to 360°

Upon entry into the C40 or C100 boundary, the radar data calculates each aircraft's entry angle and assigns it to the corresponding sector. This information is essential for determining the unimpeded time and optimizing runway assignment and sequencing.

4.2.3 Additional Time in the Terminal Area

The key performance indicator KPI08, defined as the "Additional Time in the Terminal Area" is a crucial metric for assessing the model's effectiveness in optimizing aircraft sequencing and runway utilization. KPI08 quantifies the time an aircraft spends within the terminal control area (TMA) beyond the optimal, unimpeded transit time, thereby offering insights into the efficiency of arrival sequencing and flow management (DECEA, 2020b).

This indicator is calculated as the difference between the actual time an aircraft spends in the TMA and the unimpeded time. A positive KPI08 value indicates that the aircraft experienced delays, while a negative value suggests an advance relative to the target time. For this study, KPI08 serves as an essential parameter, allowing the model to assess the degree and nature of deviations from the unimpeded time.

In our model, minimizing both delays and advances was assigned equal weight, meaning the model treats deviations from the target time symmetrically, regardless of direction. This approach enables the model to focus on reducing overall deviations from KPI08, aiming to bring each aircraft's transit time as close as possible to the unimpeded time.

4.2.4 Earliest and latest landing times

The estimation of the earliest and latest landing times presents a significant challenge due to the absence of publicly available data on key operational parameters, such as the amount of fuel carried by each aircraft and the maximum achievable velocities. These variables, which influence the aircraft's optimal speed and flight behavior, are proprietary to airlines and are not accessible through public sources. As a result, the precise calculation of the earliest and latest landing times is not feasible.

To address this limitation, this study employed an estimation approach based on historical flight data. Specifically, data from the BIMTRA database for 2023 was utilized, categorizing flights by aircraft model. A total of 256 distinct aircraft models landed at Guarulhos International Airport during this period, providing a broad dataset for analysis.

For each aircraft model, the 90th percentile of both positive and negative KPI08 values was calculated from all flights in 2023. These percentiles were used as indicators of maximum observed delay and maximum advance for each model, respectively. Using these values, the earliest and latest feasible landing times were estimated for each flight.

With this approach the model can simulate feasible landing schedules that reflect observed performance patterns while accommodating real-world operational variability.

4.2.5 Minimum Separation Times

The classification of aircraft for minimum separation purposes is defined according to wake turbulence categories, as specified in Brazilian air traffic regulations, in alignment with ICAO standards (DECEA, 2020a). These categories are based on the aircraft's maximum certified takeoff weight and are outlined as follows:

- **Super (J)**: Aircraft types specified in ICAO Document 8643 (*Aircraft Type Designators*) as "Super," such as the Airbus A380, which generate substantial wake turbulence.

- **Heavy (H)**: Aircraft with a maximum takeoff weight of 136,000 kg or more, except those classified as Super. This category includes large commercial jets that produce considerable wake turbulence.

- **Medium (M)**: Aircraft with a maximum takeoff weight below 136,000 kg and above 7,000 kg, encompassing most commercial airliners and some smaller jets, with moderate wake turbulence generation.

- **Light (L)**: Aircraft with a maximum takeoff weight of 7,000 kg or less, typically small private planes that produce minimal wake turbulence.

The separation requirements for these categories are detailed in Table 4.1, specifying the minimum separation times between leading and trailing aircraft in different categories. In cases where no specific separation time is indicated, the minimum radar separation for terminal area of 3 nautical miles is applied. This data, along with the classification guidelines, is sourced from DECEA's regulatory document on air traffic control procedures (DECEA, 2020a).

TABLE 4.1 – Separation Requirements in seconds for Landing Aircraft.

		Trailing Aircraft			
		Super	Heavy	Medium	Light
Leading Aircraft	Super	-	120	180	240
	Heavy	-	-	120	180
	Medium	-	-	-	180
	Light	-	-	-	-

4.2.6 Data Retrieval Process

This section outlines the steps taken to retrieve and process data for each parameter required in the model:

1. **Radar Detection:** Flights entering the C40 or C100 boundary were identified using radar data, capturing their entry coordinates, entry time, and flight ID.

2. **Calculation of Sector of Entrance and Distance from Airport:** The entry angle and distance of each aircraft from the airport were calculated based on its coordinates obtained from the radar data.

3. **Retrieval of Flight Information:** The flight ID was used to query the BIMTRA table to obtain additional flight details, including the target runway, wake turbulence category, aircraft model, and KPI08 value.

4. **Retrieval of Maximum Delay and Advance:** Maximum allowable delay and advance times for each aircraft model were retrieved from historical data based on similar flights, as outlined in previous sections.

5. **Calculation of Unimpeded Time for C40 or C100:** The unimpeded time was calculated according to the sector of entrance, aircraft size, and assigned runway, following the statistical analysis guidelines. When required, interpolation was applied to estimate times between predefined distances.

6. **Final Preparation for Optimization:** All necessary flight information was compiled and added to the list of active flights, preparing the dataset for the optimization process.

4.3 Testing the Model

To evaluate the model's performance, as previously mentioned, we conducted four distinct tests:

1. Feasibility Test;
2. Efficacy Test without Threshold Change;
3. Efficacy Test with Threshold Change;
4. Efficacy Test on the Busiest Days.

The Feasibility Test aimed to evaluate the model's viability in optimizing aircraft sequencing under real-world operational conditions. This test was conducted during the peak traffic period on October 5, 2023, from 09:00 to 11:00. According to the histogram in Figure 4.3, this period illustrates a high demand scenario.

For the Efficacy Test without Threshold Change, we selected three days with favorable meteorological conditions and traffic volumes at or above the annual average, which was 15.79 landings per hour in 2023. The selected days and traffic details were as follows:

- January 28, 2023, from 08:00 to 10:00, with 21 landings during the 08th hour and 24 landings during the 09th hour.
- March 21, 2023, from 18:00 to 20:00, with 17 landings during the 18th hour and 19 landings during the 19th hour.
- April 24, 2023, from 08:00 to 10:00, with 20 landings during the 08th hour and 24 landings during the 09th hour.

For the Efficacy Test with Threshold Change, we selected three dates where runway threshold direction changes occurred, alongside traffic volumes meeting or exceeding the annual average. The selected dates and traffic conditions, referring to planes landing within each hour, were as follows:

- March 1, 2023, from 18:00 to 20:00, with 16 landings during the 18th hour, 17 landings during the 19th hour, and a threshold change at 18:18:23.

- March 29, 2023, from 15:00 to 17:00, with 20 landings during the 15th, 18 landings during the 16th hour, and a threshold change at 15:26:20.

- May 20, 2023, from 19:00 to 21:00, with 27 landings during the 19th, 18 landings during the 20th hour, with a threshold change at 19:24:30.

Lastly, for the Efficacy Test conducted on the busiest days, we selected the three highest-traffic days of the year during their busiest hour, allowing us to analyze the model's performance under maximum demand conditions:

- October 5, 2023, during the 10th hour, as shown in the histogram in Figure 4.3.

- September 13, 2023, during the 10th hour, as shown in the histogram in Figure 4.4.

- December 1, 2023, during the 10th hour, as shown in the histogram in Figure 4.5.

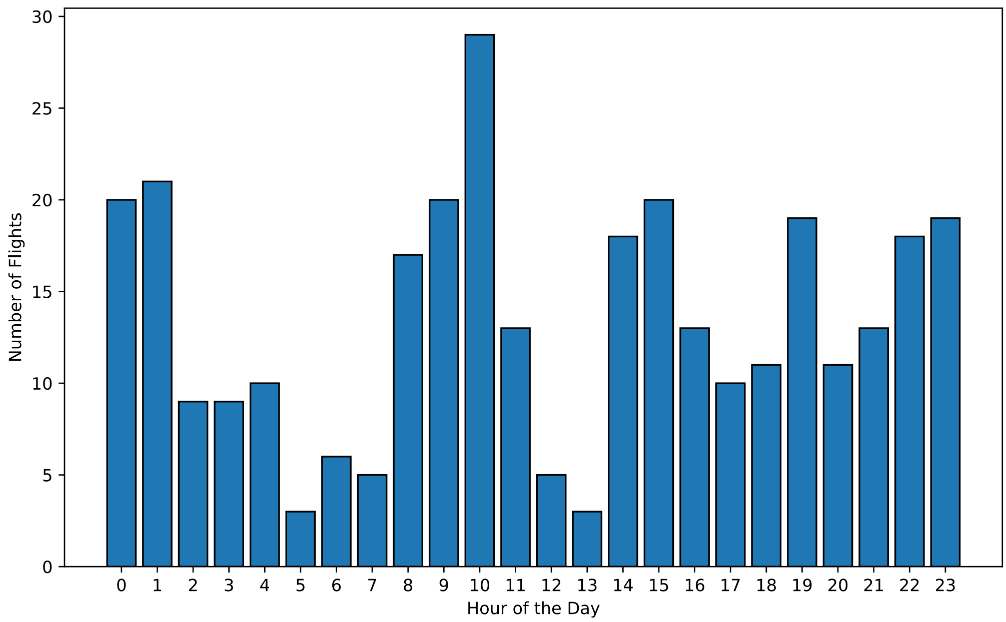

FIGURE 4.3 – Histogram of flights by hour on October 5, 2023.

These histograms help visualize the peak traffic periods within each hour, illustrating the high-demand scenarios that challenge the model. Each test was designed to evaluate the model s capacity to provide timely sequencing optimizations and its practical application in managing aircraft delays and advances under realistic operational conditions. In the next chapter, we will delve into the details of how these tests were conducted.

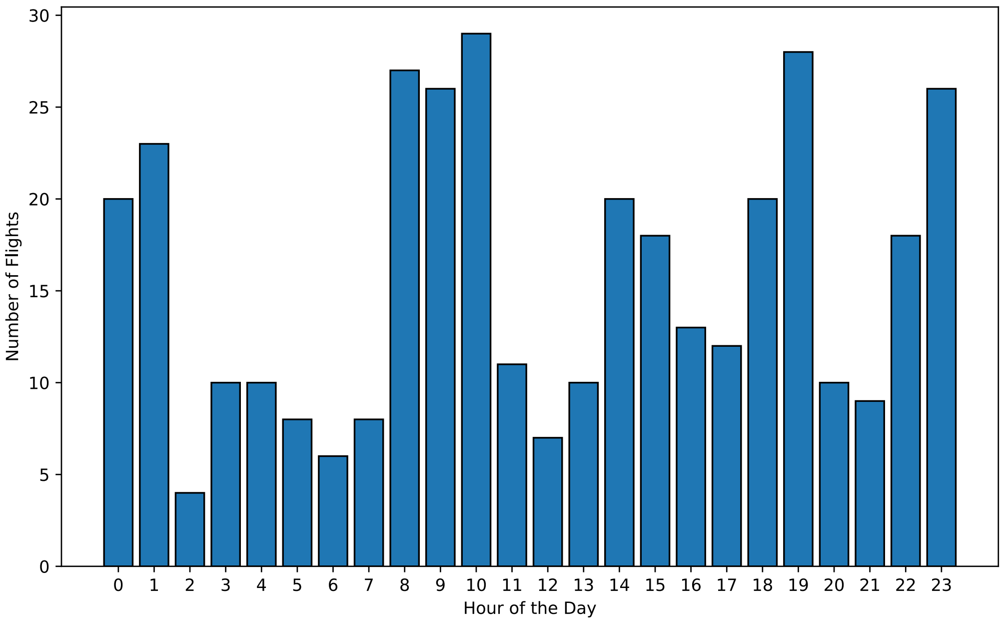

FIGURE 4.4 – Histogram of flights by hour on September 13, 2023.

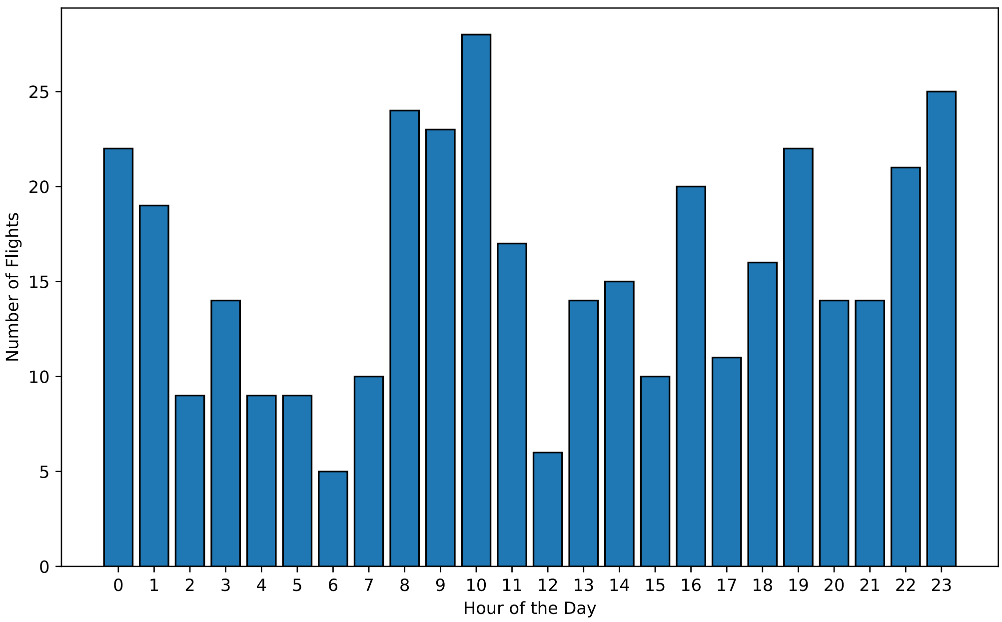

FIGURE 4.5 – Histogram of flights by hour on December 12, 2023.

5 Detailed Testing Methodology

In this chapter, we provide a detailed explanation of the tests conducted and outline the approach used to evaluate their results.

5.1 Feasibility Test

The feasibility test was designed to evaluate whether the proposed model could generate an optimized landing sequence within a practical time frame, thereby confirming its suitability for managing the complexities of real-time flight operations.

To conduct this evaluation, we queried the BIMTRA table to retrieve the full set of flight records for 2023, allowing us to identify the day with the highest recorded number of arrivals at GRU. October 5, 2023, emerged as the busiest day, making it the primary test date for our analysis. According to the histogram in Figure 4.3, the interval from 09:00 to 11:00 was identified as the period with the highest volume of flights, making it the focus for this analysis. This peak period provides a critical window for examining the model's performance in high-demand conditions. Once identified, radar data corresponding to this interval was filtered for flights entering two designated airspace boundaries around Guarulhos International Airport (GRU): C40 (test 1) and C100 (test 2). By applying these two test conditions, the study captures the model's adaptability to both closer, immediate airspace (C40) and an extended perimeter (C100), examining its feasibility across varying distances from the airport.

In this algorithm, a list of active flights is maintained and continuously updated. The algorithm scans each radar update to identify new flights entering the designated boundaries, as well as flights that no longer appear in the radar feed. If a flight is absent in subsequent radar intervals, this absence is interpreted as either a landing or an exit from the designated airspace, resulting in its removal from the active flights list.

Given that the radar may sometimes miss an aircraft momentarily, a flight is only marked as inactive if it fails to appear for five consecutive updates, which is equivalent to 20 algorithm iterations. Each new flight detected within the specified radius is promptly added to the active flights list for the respective test.

For each newly detected flight, the algorithm triggers the optimization routine for all active flights. For each active flight, the model retrieves essential data, accordingly to the methodology described in Section 4.2.6. After gathering this data for all active flights, the optimization routine executes, aiming to produce a coordinated landing sequence that meets operational requirements and optimizes the flow of incoming flights.

This structured test setup, with a real-time data simulation, validates the feasibility of the model under realistic peak-traffic scenarios at different distances from the destination. By testing the model's responsiveness and effectiveness within both the C40 and C100 boundaries, we demonstrate its potential for deployment in real-time air traffic management, capable of handling dynamically shifting data and adjusting landing sequences to maintain optimal airport operations.

5.2 Efficacy without Threshold Change Test

The efficacy test aimed to evaluate the model's performance in optimizing landing sequences by comparing its recommendations with actual operational data, in both C40 and C100 scenarios. This test specifically focused on a no-threshold-change scenario, assessing the cumulative additional time spent in the terminal area, i.e. the KPI08, by comparing model-calculated values with the real-world KPI08 values recorded in the BIMTRA table. This comparison provided insight into whether the model's suggested adjustments for delaying or advancing landing times led to measurable improvements in reducing extended times within terminal airspace.

The specific periods specified in Section 4.3 were selected to simulate aircraft trajectories. To ensure a fair comparison with real-world conditions, the simulation periods were chosen to exclude threshold changes and significant weather disruptions that could impact flight patterns. METAR data, which provides hourly meteorological reports at airport terminals, was consulted to verify that conditions were consistently clear, with CAVOK (Ceiling and Visibility OK) entries indicating favorable conditions devoid of weather-related disturbances.

5.2.1 Model Simulation

In order to obtain models's optimized KPI08 values, we simulated aircraft trajectories for the defined periods, covering the complete trajectory of each plane from the time it first appeared in radar data until landing in the simulation. The focus was specifically on capturing the initial radar detection for each plane; this initial detection served as the starting point for the simulated trajectory. As new flights entered the designated radar boundaries — C40 and C100 — they were added to a list of active flights, and relevant data was retrieved, as outlined in Section 4.2.6.

Our simulation assumed that each aircraft would adhere precisely to the model's recommendations, implementing any delay or advance linearly. Upon identification of a new flight, the model set its estimated time of arrival to the unimpeded time, as defined in previous sections. For all previously detected active flights, their ETAs were kept at the initially identified unimpeded time, as the goal was to minimize deviations from this original estimate.

Every time a new aircraft was identified, the optimization algorithm generated an updated landing time for each active flight, which represented the time each plane would land if it followed the model's recommendations. When the optimized landing time for any flight matched the total elapsed time in the simulation, it indicated that the plane had landed. The plane was then removed from the active list, and its KPI08 value was calculated by subtracting its unimpeded time from its actual landing time.

The test continued beyond the period covered by the radar data, running optimizations until all identified flights within that period had completed their trajectories.

5.2.2 FCFS Model

For the real flights data, even within the selected periods, there may be additional operational factors — such as takeoff operations — that impact the recorded KPI08 values, making them less than ideal for direct comparison. To ensure a fair evaluation against our model, we implemented a FCFS model, which provides a baseline sequence for arriving planes by prioritizing them in the obvious order of their ETAs.

The FCFS model maintains aircraft in the order of their updated ETAs, applying delays only when necessary to meet minimum separation requirements. This simple sequencing method offers a straightforward comparison for assessing the benefits of our model's optimized sequencing approach. The same simulation process, as previously described, was applied to the FCFS model to generate its KPI08 values, providing a consistent basis for comparison with both the real radar data and our optimized model.

5.2.3 Evaluation

To assess the efficacy of our approach, we compared three cases: the real-world KPI08 values from the BIMTRA table, the FCFS baseline model, and our optimized MIP model. For each flight within the selected periods, we calculated the KPI08 values for each model in both the C40 and C100 scenarios. We then summed the absolute KPI08 values separately for each scenario, yielding cumulative KPI08 scores for each period. This cumulative metric allowed us to quantify each model's ability to minimize deviations from unimpeded times in terminal airspace by comparing it directly to both real-world data and the FCFS baseline.

To ensure an accurate comparison, we chose not to include KPI08 values for aircraft already within the radar's range at the start of the simulation. For these flights, the KPI08 would reflect only the additional time spent in a smaller area than the full 40 or 100 NM boundary as recorded in BIMTRA, since they were already within the designated airspace. Consequently, our comparison focused solely on aircraft that entered the boundary after the start of the simulation.

5.3 Model Efficacy with Threshold Change

This efficacy test followed a similar approach to the previous methodology but introduced an additional operational variable: threshold changes. These changes, typically implemented in response to factors such as wind direction or traffic flow, significantly impact landing sequences by altering the approach paths that incoming aircraft must follow. This test was also conducted for both C40 and C100 scenarios to assess the model's adaptability across varying operational conditions.

The objective of this test was to evaluate the model's capacity to manage landing sequences efficiently when threshold changes occur, incorporating advance notice for each shift. By simulating the model's response with 15 minutes of lead time for each threshold change — consistent with GRU's operational protocols — we aimed to measure the potential benefits of threshold awareness in optimizing landing sequences. While this 15-minute notice exists in GRU's procedures, it has not yet been implemented in actual landing operations, as discussed in previous sections.

To simulate realistic operational conditions, the three periods with documented threshold changes specified in Section 4.3 were selected, each presenting a scenario where the model would have advance knowledge of these shifts. We identified periods with threshold changes in the BIMTRA table by observing consecutive flights with differing landing thresholds, indicating an adjustment in the designated landing points on the runway.

Unlike the previous efficacy test, this simulation did not prioritize selecting days with CAVOK conditions in the METAR data, as threshold changes often coincide with challenging meteorological situations. Although this variability may introduce minor inconsistencies when comparing with real-world data — especially since our model does not account for meteorological conditions – the test still provides valuable insights into the advantages of advanced threshold awareness.

5.3.1 Model Simulation

This simulation required additional data beyond the initial efficacy test, specifically the ETAs for both the active and upcoming thresholds. With ETAs available for both configurations, the model could dynamically adjust each aircraft's approach to align with the anticipated threshold change, optimizing sequencing for both the current and updated landing configurations.

Similar to the previous test, upon identifying a new flight, the model set its ETAs to both of the thresholds to the unimpeded times, as defined in previous sections. For all previously detected active flights, their ETAs were kept at the initially identified unimpeded times to minimize any deviations from this original estimate.

Each new optimization updated aircraft trajectories based on the latest optimization results. Whenever a threshold change was scheduled, the model recalculated each aircraft's ETA to account for the new landing configuration. To ensure consistency when the threshold changed, each aircraft was assumed to retain the same entry sector used when crossing the selected boundary (C40 or C100) throughout its trajectory.

Once again, the test continued beyond the radar data period, running optimizations until all flights identified in that period had landed, ensuring a comprehensive analysis of each plane's complete trajectory within the test window.

5.3.2 FCFS model

To provide a fair baseline for comparison, we also included an FCFS model under the same threshold-aware environment as our optimized model, with advance knowledge of threshold changes 15 minutes before they occurred. The FCFS model sequenced aircraft based solely on their initial ETAs, applying delays only to meet minimum separation requirements, without further optimization.

For flights whose delayed landing times extended beyond the threshold change, the FCFS model reordered these flights based on their ETAs for the new threshold, again applying delays as needed to ensure minimum separation. This approach allowed the FCFS model to adapt to the threshold change while maintaining a straightforward sequencing order.

The same simulation process was applied to the FCFS model, ensuring that both the baseline and the optimized model generated KPI08 values under equivalent conditions.

5.3.3 Evaluation

The evaluation followed the same methodology as the previous efficacy test, comparing the real-world KPI08 values from the BIMTRA table, the FCFS baseline model, and our optimized MIP model. This analysis was conducted across the selected periods and for both C40 and C100 scenarios, providing a comprehensive comparison of each model's performance in managing landing sequences under threshold change conditions.

5.4 Efficacy Test in Busiest Days

This test closely follows the methodology outlined in Section 5.2, where the model's efficacy was evaluated without considering threshold changes. However, in this case, we focused on the busiest days of the year to assess the model's performance under peak traffic conditions. By selecting periods with maximum operational load, this test aims to determine how effectively the model manages landing sequences when airspace demand is at its highest.

For this analysis, we also tested both the C40 and C100 scenarios. Unlike the previous efficacy test, we chose not to factor in METAR data or weather conditions, as the objective here was to assess the model's performance specifically under heavy traffic. Consequently, real-world KPI08 values from the BIMTRA dataset were excluded from this comparison. Instead, we focused solely on comparing the model's optimized solutions to the FCFS baseline. Peak traffic conditions inherently increase the likelihood of the optimized model outperforming the FCFS approach, making this an effective setup to observe any potential advantages.

Additionally, as this comparison did not involve real-world data, KPI08 values for aircraft already within radar range at the start of the simulation were included in the analysis.

6 Results

In this chapter, we present and discuss the results obtained in the experiments conducted to evaluate the proposed model's performance.

6.1 Models Comparison

The results obtained from the comparison between the two models presented in this study, following the methodology outlined in Section 4.1, are shown in Table 6.1.

TABLE 6.1 – Comparison of execution time, value, number of constraints and variables between the Classic Model and Our Model for different values of N and R.

		Classic Model				Our Model			
N	R	Time (s)	Value	Constraints	Variables	Time(s)	Value	Constraints	Variables
10	1	0.0392	700	600	240	0.0670	700	334	151
	2	0.0266	90	755	250	0.1177	90	558	272
	3	0.0110	0	910	260	0.0803	0	782	393
15	1	0.4859	1480	1275	510	1.5036	1480	649	301
	2	0.0864	210	1620	525	0.5821	210	1133	557
	3	0.0251	0	1965	540	0.2485	0	1617	813
20	1	0.1192	820	2200	880	1.3861	820	1064	501
	2	0.0611	60	2810	900	0.7175	60	1908	942
	3	0.0317	0	3420	920	0.0991	0	2752	1383
30	1	0.0175	24442	4800	1920	0.1115	24442	2194	1051
	2	0.2422	554	6165	1950	0.6749	554	4058	2012
	3	0.0338	0	7530	1980	0.3089	0	5922	2973
44	1	0.2064	1550	10120	4048	0.6220	1550	4448	2157
	2	0.0987	0	13046	4092	0.2006	0	8412	4182
	3	0.0599	0	15972	4136	0.2219	0	12376	6207

We can observe that both models found the optimal solution for all test instances. However, the classic model consistently achieved the optimal solutions with considerably shorter execution times than those required by the proposed model.

The disparity in execution times likely stems from the differences in the number of constraints and variables each model employs. Specifically, the classic model utilizes more constraints, many of which are valid inequalities. These constraints effectively reduce the solution space, thereby accelerating the convergence to optimal results.

Additionally, another factor that may have contributed to the difference in execution times is the rapid increase in the number of variables as the number of runways expands. In our proposed model, the binary variable count scales linearly with the number of runways, while in the classic model, this growth is much more gradual. This configuration leads to increased computational demands, particularly as the number of runways grows.

In conclusion, the findings highlight the need for further refinement of the proposed model to enhance its computational efficiency and scalability.

6.2 Feasibility Test

We performed the feasibility test according to the methodology described in Section 5.1 for both the C40 and C100 scenarios. In the following sections, we present the results obtained.

6.2.1 C40 Scenario

Table 6.2 summarizes the optimization results for the C40 scenario based on radar data collected during the 10th hour of October 5, 2023. For each new aircraft detected in the radar data, the model was triggered to perform an optimization, with each row representing one of these optimization instances. The table lists the number of active planes at the time of each optimization, the timestamp, the model's computation time (in seconds), and the number of iterations required to reach a solution.

The results show strong consistency, with all computation times remaining below 1 second, even as the number of active planes fluctuated. Notably, at the peak of 15 active planes, the model maintained efficient processing times, with computation times increasing slightly but still within operational limits. This peak represents the highest workload during the test period, demonstrating the model's robustness and its capacity to adapt to elevated traffic levels without compromising performance.

These findings indicate that the model is well-suited for real-time application in managing air traffic, consistently generating optimized landing sequences in a timely manner, regardless of traffic intensity variations within the C40 airspace.

TABLE 6.2 – Optimization results for the C40 scenario based on radar data from October 5, 2023, during the 10th hour.

#	Active Planes	Time	Model Time (s)	Iterations
1	10	10:00:01	0.0202	57
2	10	10:01:14	0.0194	52
3	10	10:01:30	0.0147	60
4	11	10:02:34	0.0696	200
5	12	10:03:30	0.2678	1644
6	13	10:05:22	0.1810	687
7	14	10:05:26	0.6264	6165
8	13	10:06:59	0.2828	1808
9	14	10:07:39	0.5976	2338
10	15	10:08:07	0.7523	22445
11	13	10:09:00	0.8629	11759
12	14	10:09:24	0.9434	25024
13	14	10:12:08	0.8566	14625
14	15	10:13:29	0.9248	29738
15	15	10:15:41	0.5640	5659
16	14	10:16:17	0.2285	1435
17	9	10:20:54	0.0379	110
18	11	10:21:14	0.1595	793
19	13	10:21:54	0.3977	16106
20	13	10:24:10	0.3468	2321
21	12	10:26:39	0.4165	2837
22	11	10:27:23	0.0262	47
23	12	10:28:04	0.0394	71
24	13	10:28:56	0.0442	106
25	12	10:29:20	0.1417	252
26	13	10:30:00	0.6039	5028
27	13	10:31:24	0.4399	3476
28	14	10:32:24	0.2597	1796
29	12	10:34:21	0.0424	114
30	13	10:34:49	0.2619	1472
31	12	10:36:05	0.0552	156
32	12	10:36:57	0.1034	168
33	10	10:42:54	0.0320	73
34	10	10:47:19	0.1139	1009
35	8	10:50:40	0.0147	28
36	8	10:53:44	0.0077	18
37	7	10:57:13	0.0062	9
38	7	10:59:33	0.0062	9

6.2.2 C100 Scenario

Table 6.3 shows the optimization results for the C100 scenario based on radar data from October 5, 2023, during the 10th hour. Compared to the C40 scenario, this table has fewer rows, as the C100 airspace initially contains more active planes, resulting in fewer new aircraft entering the area over time. Despite this difference, we observe that the number of active planes per optimization is generally higher in the C100 scenario, with peaks reaching up to 21 planes.

In contrast to the C40 scenario, where optimization times remained consistently below 1 second, the C100 scenario exhibited greater variability in computation times, with a peak of 251 seconds (approximately 4 minutes) observed during the highest traffic density. This increase in processing time can be attributed to the higher number of active planes and the associated complexity of sequencing under such conditions. While this result implies that the model may experience longer processing times under intense traffic, it remains within acceptable operational limits, especially considering that in practice, optimization does not need to be triggered with each incoming aircraft but rather at strategically spaced intervals.

These findings suggest that while the current optimization model is effective in handling dense airspace configurations, further research into heuristic methods may be beneficial to enhance processing efficiency, especially with anticipated increases in air traffic. Heuristic techniques could provide approximate solutions more quickly, enhancing the real-time applicability of the model under even denser traffic conditions.

Overall, the model's ability to complete optimizations within an acceptable time frame, even at peak demand, reinforces its viability as a robust solution for air traffic management. Its successful handling of high-density scenarios highlights its potential as a scalable tool that can support air traffic sequencing and management in increasingly complex airspace environments, ensuring timely optimization for future applications.

TABLE 6.3 – Optimization results for the C100 scenario based on radar data from October 5, 2023, during the 10th hour.

#	Active Planes	Time	Model Time (s)	Iterations
1	19	10:00:01	0.1737	3458
2	19	10:00:42	0.1473	2119
3	19	10:02:02	1.8161	193410
4	20	10:03:14	18.7124	1817542
5	19	10:09:36	7.4241	978640
6	20	10:10:00	45.9543	4807208
7	21	10:13:29	259.3412	26059171
8	21	10:15:37	17.0966	1741582
9	20	10:18:30	0.4417	21301
10	19	10:20:38	6.2966	575847
11	20	10:23:14	0.6574	56799
12	20	10:24:51	17.6923	1268791
13	20	10:27:03	7.6848	646263
14	18	10:30:40	2.5983	207206
15	15	10:38:45	0.0164	88
16	13	10:43:34	0.0244	114
17	13	10:46:03	0.0388	168
18	13	10:48:11	0.0597	741
19	14	10:48:23	0.0576	732
20	12	10:52:56	0.0083	36
21	13	10:54:56	0.0059	21
22	12	10:57:33	0.0056	20

6.3 Efficacy without Threshold Change Test

This section presents the results of the efficacy test for a no-threshold-change scenario, accordingly to the methodology described in Section 5.2, comparing the optimized model's performance against both the FCFS baseline and actual KPI08 values from BIMTRA data across the selected periods.

6.3.1 C40 Scenario

The comparison results for January 28, March 21, and April 24, 2023, in the C40 scenario are shown in Figures 6.1 to 6.3. In these figures, aircraft are displayed in the legend according to their landing order based on the FCFS baseline sequence. Lines connecting the points on both our model and FCFS represent the landing sequence within each model, illustrating the order in which aircraft were scheduled to land. Figure 6.4 synthesizes these results by presenting the cumulative absolute KPI08 values for each case across the three days.

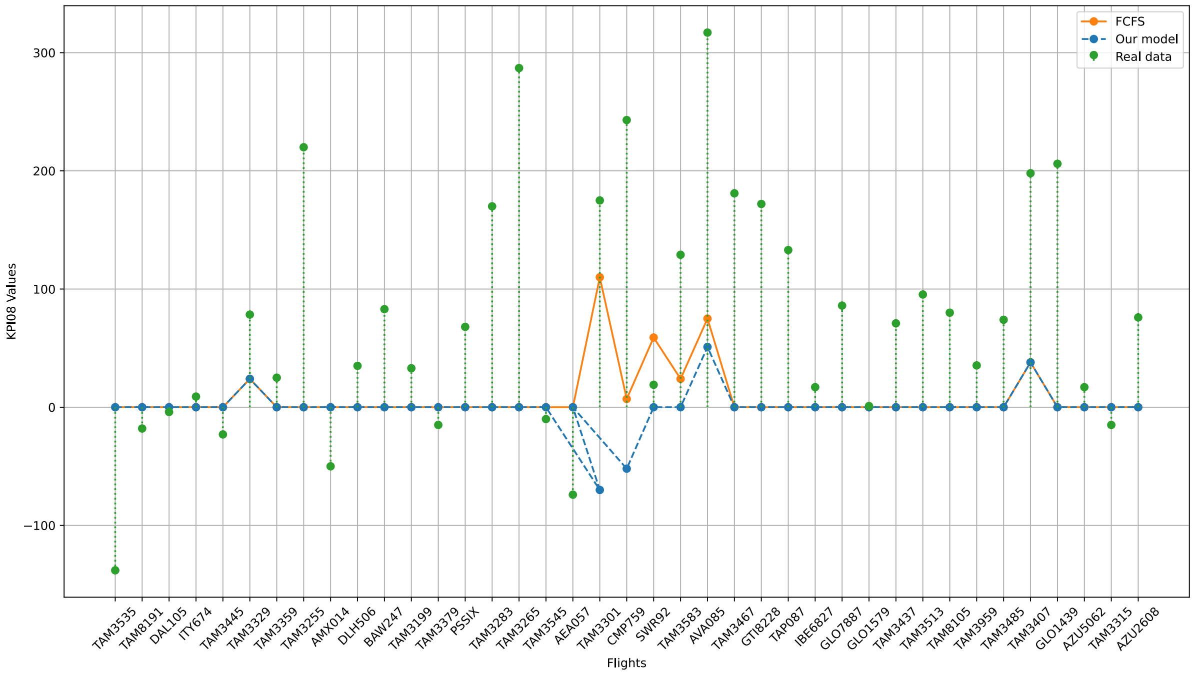

FIGURE 6.1 – KPI08 comparison for January 28, 2023, during the 08:00 to 10:00 period in the C40 scenario.

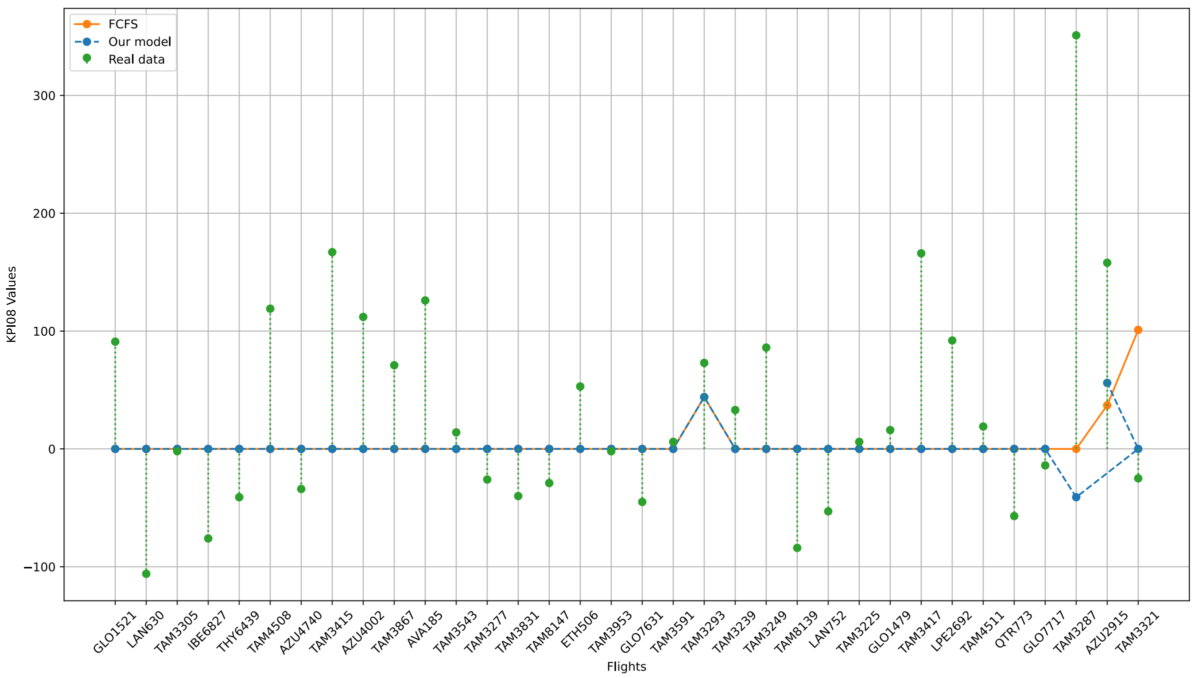

FIGURE 6.2 – KPI08 comparison for March 21, 2023, during the 18:00 to 20:00 period in the C40 scenario.

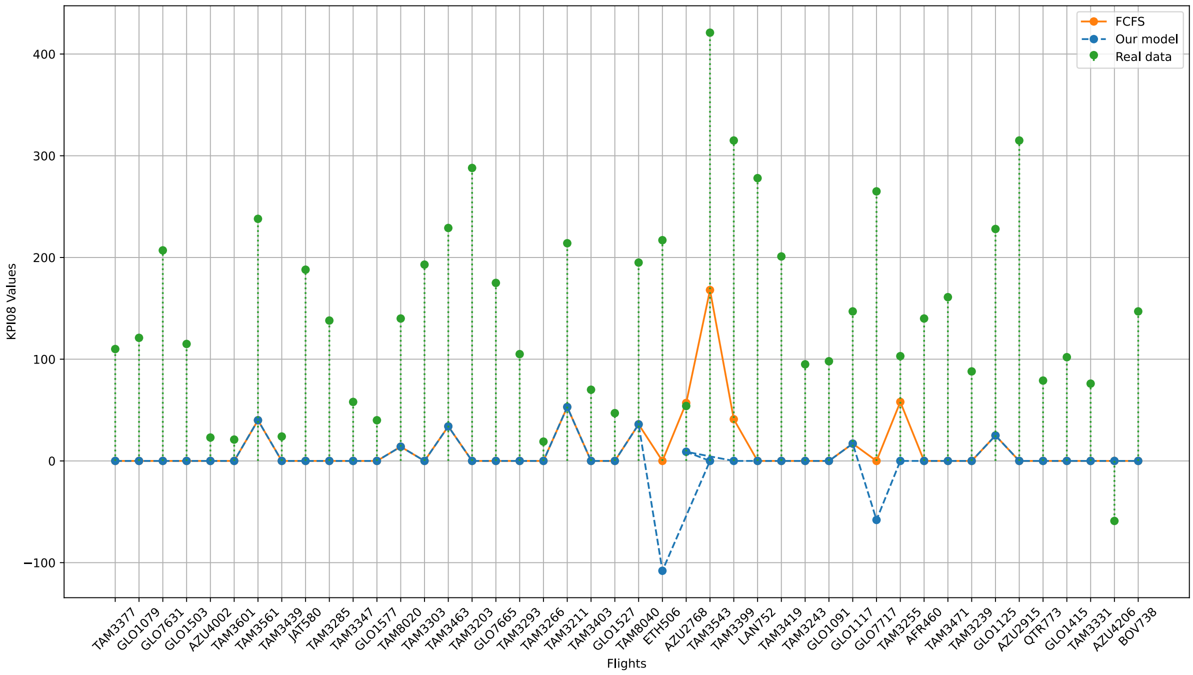

FIGURE 6.3 – KPI08 comparison for April 24, 2023, during the 08:00 to 10:00 period in the C40 scenario.

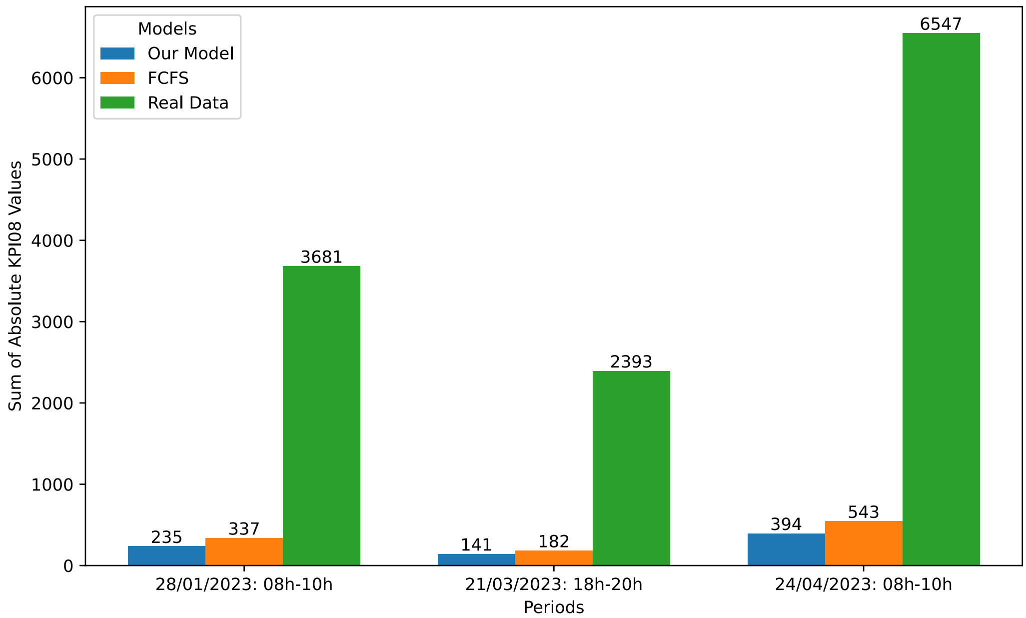

FIGURE 6.4 – Cumulative absolute KPI08 values for January 28, March 21, and April 24, 2023, in the C40 scenario.

The optimized model demonstrates significant efficacy in reducing cumulative delays in the C40 scenario, outperforming both the FCFS baseline and real-world BIMTRA data. Notably, it achieved a remarkable 93.9% reduction in cumulative delays compared to BIMTRA data. This substantial difference is likely due to operational factors present in real-world scenarios that are not represented within the controlled simulation environment. Such factors include air traffic controller interventions, real-time adjustments, and tactical decisions that can increase cumulative KPI08 values in practice. This discrepancy underscores the importance of comparing the optimized model directly with the FCFS baseline, where both models operate under equivalent, controlled conditions.

Consistently, the optimized model outperforms the FCFS baseline by providing adjusted landing times that effectively reduce cumulative KPI08, even in scenarios without changes in landing order. This ability to optimize landing times highlights its efficiency in minimizing deviations — both delays and advances — within the terminal area and reinforces its value in enhancing air traffic sequencing.

For example, as shown in Figure 6.1, our model proposes a change in the landing order for aircraft AEA057 and TAM3301. In the FCFS model, AEA057, classified as a Heavy aircraft, lands before TAM3301, a Medium aircraft, which requires TAM3301 to maintain a minimum separation of 120 seconds from AEA057. By reordering the sequence so that TAM3301 lands 60 seconds earlier, our model reduces the necessary separation, enabling a reduction in the absolute KPI08 value. Figures 6.2 and 6.3 illustrate additional sequence changes that contribute to further KPI08 reductions.

Across the three days analyzed, the optimized model achieved an average reduction of 39.12% in cumulative deviations compared to the FCFS approach, emphasizing its significant advantage in optimizing landing times under simulated conditions.

6.3.2 C100 Scenario

The KPI08 comparison results for January 28, March 21, and April 24, 2023, in the C100 scenario are displayed in Figures 6.5 to 6.7. Similar to the C40 scenario, aircraft are listed according to the FCFS baseline sequence, with connecting lines indicating the landing sequence within each model. Figure 6.8 provides the cumulative absolute KPI08 values across the three days for this scenario.

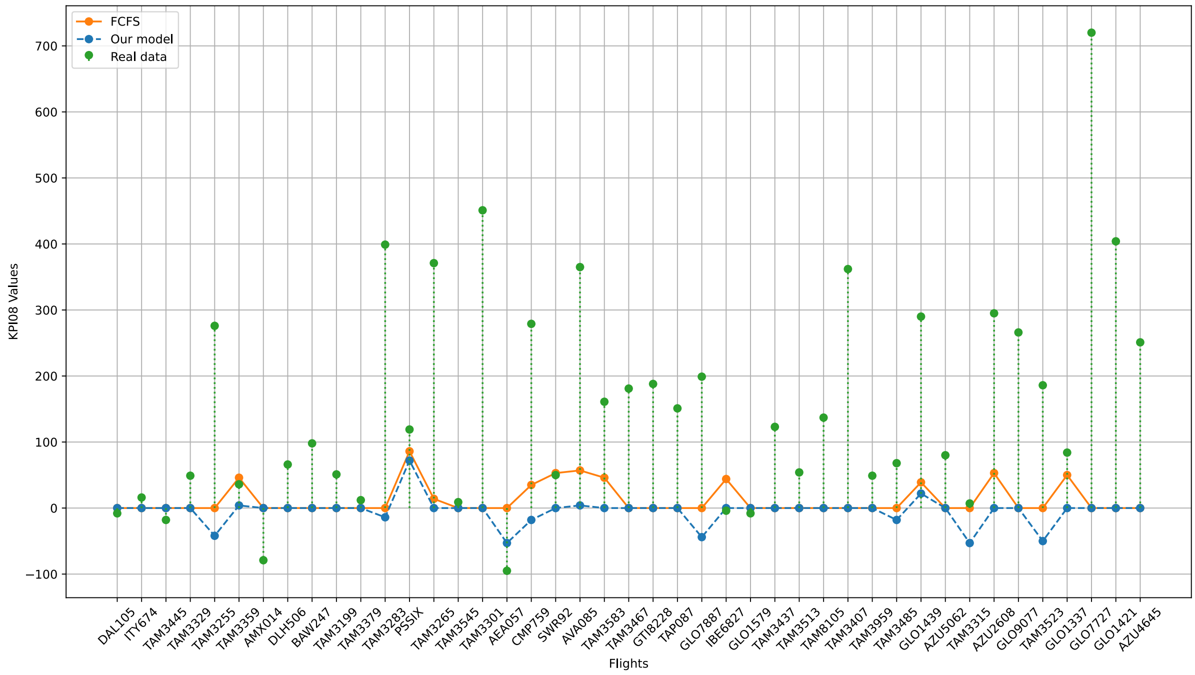

FIGURE 6.5 – KPI08 comparison for January 28, 2023, during the 08:00 to 10:00 period in the C100 scenario.

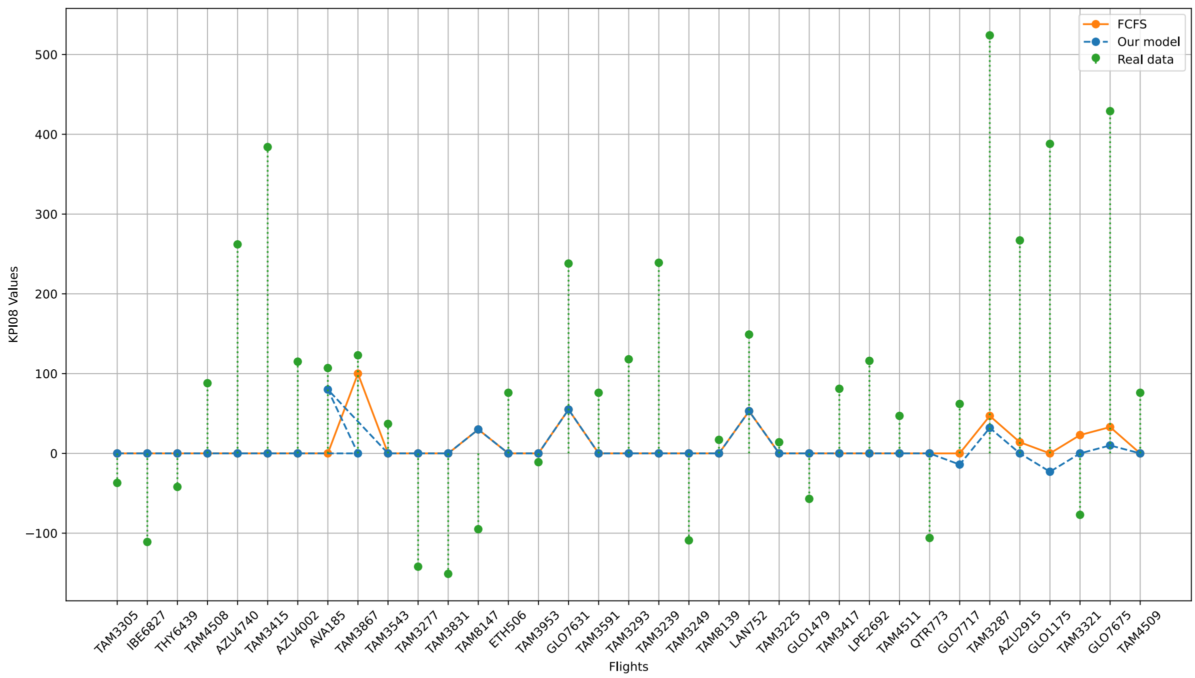

FIGURE 6.6 – KPI08 comparison for March 21, 2023, during the 18:00 to 20:00 period in the C100 scenario.

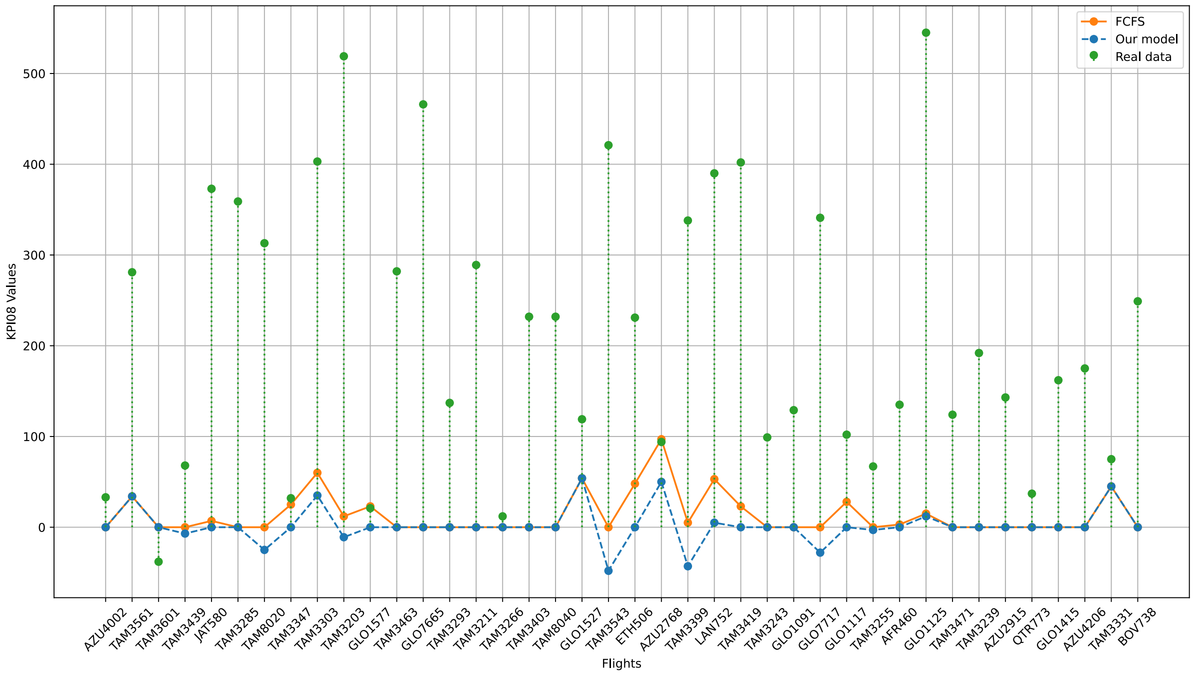

FIGURE 6.7 – KPI08 comparison for April 24, 2023, during the 08:00 to 10:00 period in the C100 scenario.

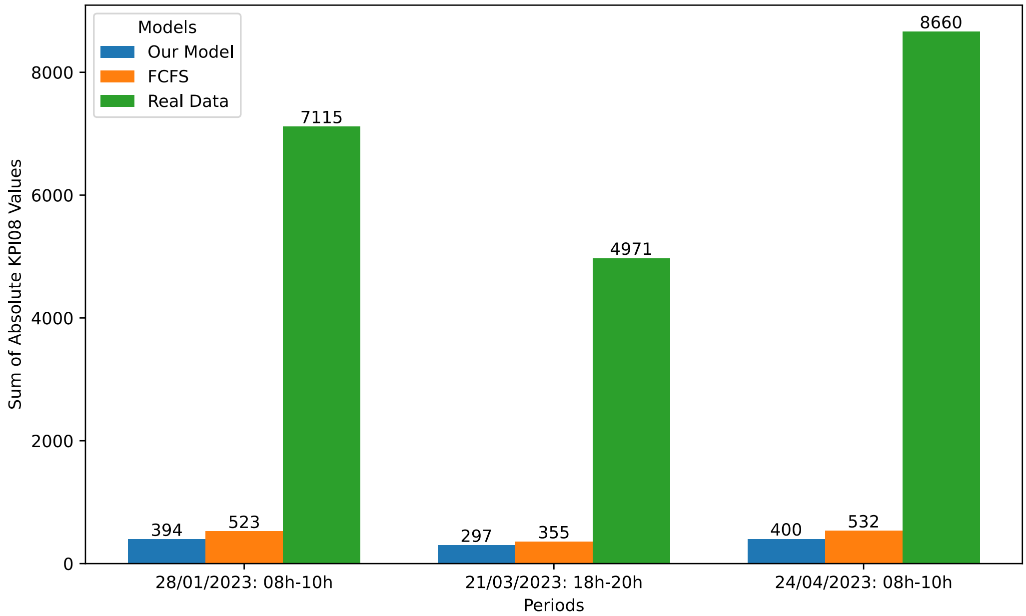

FIGURE 6.8 – Cumulative absolute KPI08 values for January 28, March 21, and April 24, 2023, in the C100 scenario.

The optimized model shows strong performance in the C100 scenario, achieving a notable reduction in cumulative deviations when compared to both the FCFS baseline and BIMTRA data. Specifically, the model reduced cumulative deviations by 94.62%

relative to BIMTRA data, under the same conditions discussed in the C40 scenario. This greater reduction, compared to the C40 results, highlights the advantage of initiating control in earlier phases.

When compared to the FCFS baseline, the optimized model achieved a more modest reduction of 22.67%. This smaller improvement reflects the conditions of the C100 scenario, where aircraft arrival times are generally more spread out, allowing fewer adjustments to reduce cumulative delays and advances in less congested settings. Furthermore, the majority of aircraft in the radar data are medium-sized, making the optimal sequence closely aligned with the FCFS sequence due to the reduced impact of sequencing on delay and advance minimization under these conditions.

Despite these limitations, the model demonstrates its adaptability by effectively adjusting landing times where sequence changes are possible and beneficial. For example, as shown in Figure 6.6, the model proposes a change in the landing order that contributes to a reduction in the absolute KPI08 value. In other cases, as illustrated in Figures 6.5 and 6.7, the model does not alter the landing order yet still achieves reductions in KPI08 by precisely adjusting landing times.

Together, the analyses of both C40 and C100 scenarios illustrate the optimized model's effectiveness in reducing cumulative deviations across different airspace configurations. The model consistently outperformed both the FCFS baseline and real-world data from BIMTRA in each scenario, demonstrating its robustness and efficiency in improving air traffic sequencing under a range of operational conditions.

6.4 Efficacy with Threshold Change Test

This section presents the results of the efficacy test conducted under conditions with threshold changes, as outlined in Section 5.3. The analysis compares the performance of the optimized model against both the FCFS baseline and KPI08 values extracted from BIMTRA data, focusing on the selected dates.

6.4.1 C40 Scenario

The results for March 01, March 29, and May 20, 2023, in the C40 scenario with threshold change are shown are shown in Figures 6.9 to 6.11. These figures display aircraft in the legend according to the FCFS baseline landing sequence, with connecting lines illustrating the sequence in both the optimized model and FCFS. In Figure 6.12, cumulative KPI08 values for each date are synthesized to provide a comparative view across the three days.

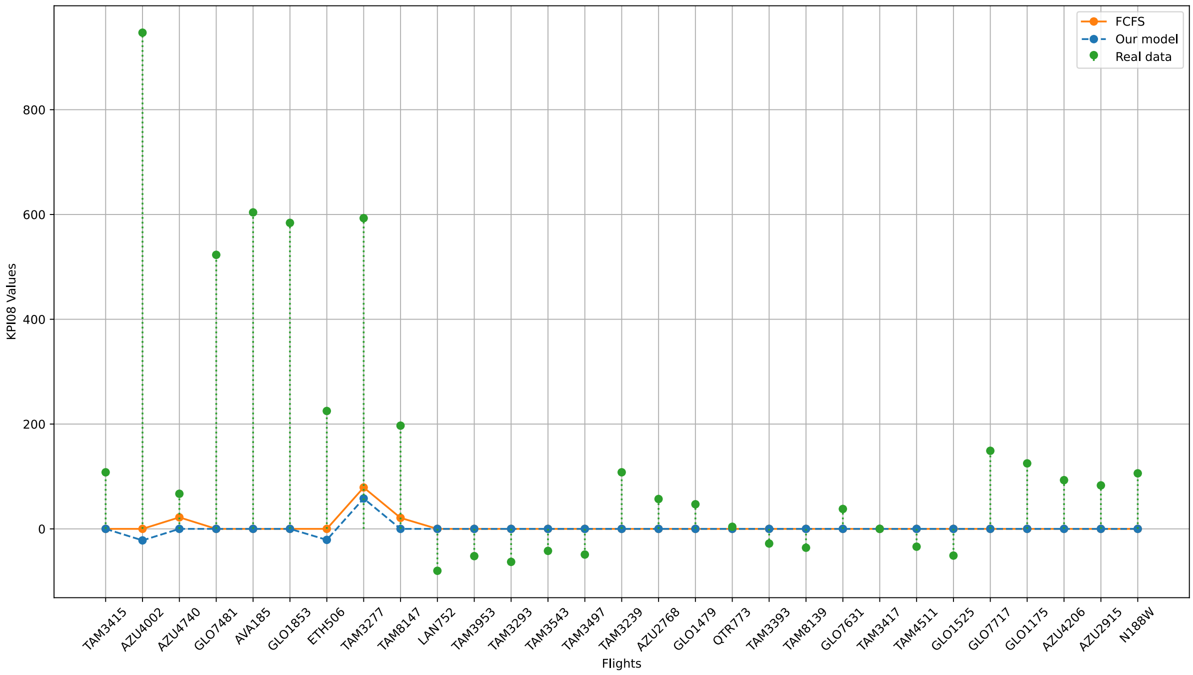

FIGURE 6.9 – KPI08 comparison for March 01, 2023, during the 18:00 to 20:00 period in the C40 scenario with threshold change.

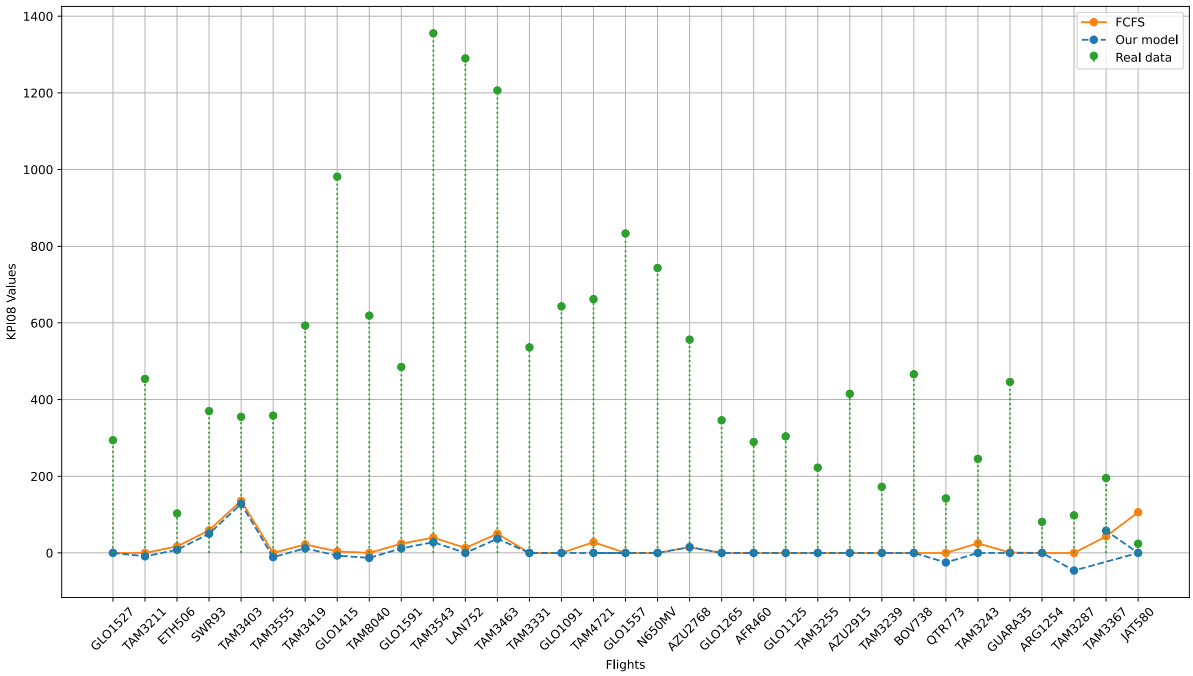

FIGURE 6.10 – KPI08 comparison for March 29, 2023, during the 15:00 to 17:00 period in the C40 scenario with threshold change.

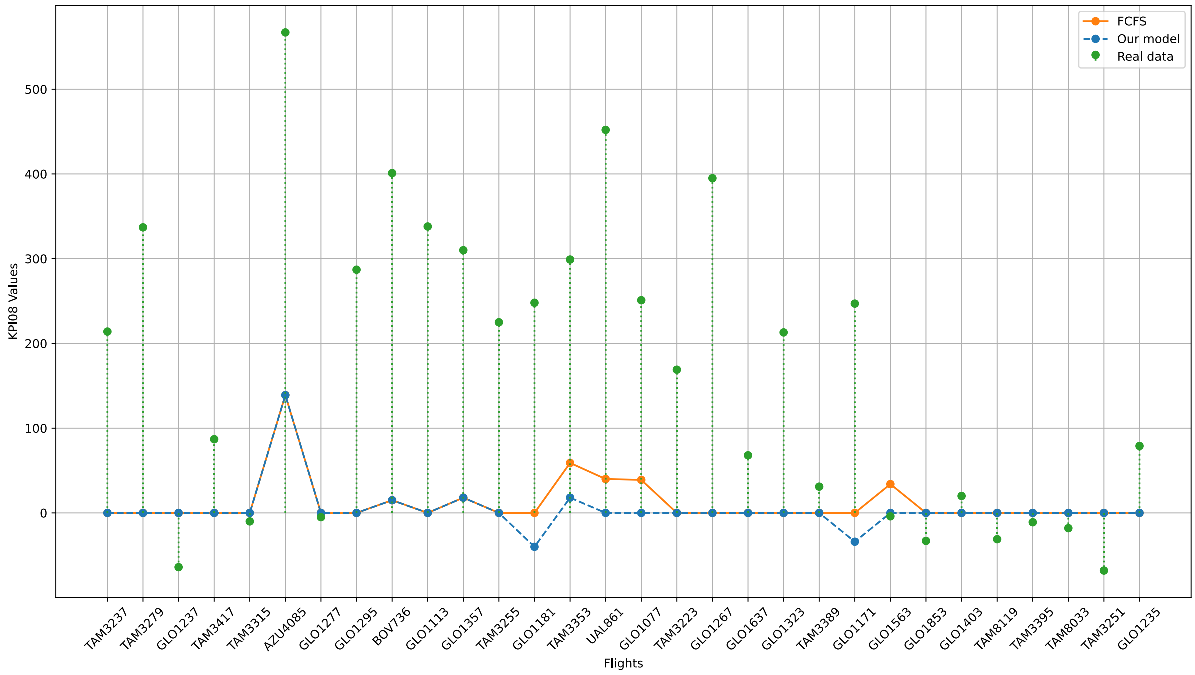

FIGURE 6.11 – KPI08 comparison for May 20, 2023, during the 19:00 to 21:00 period in the C40 scenario with threshold change.

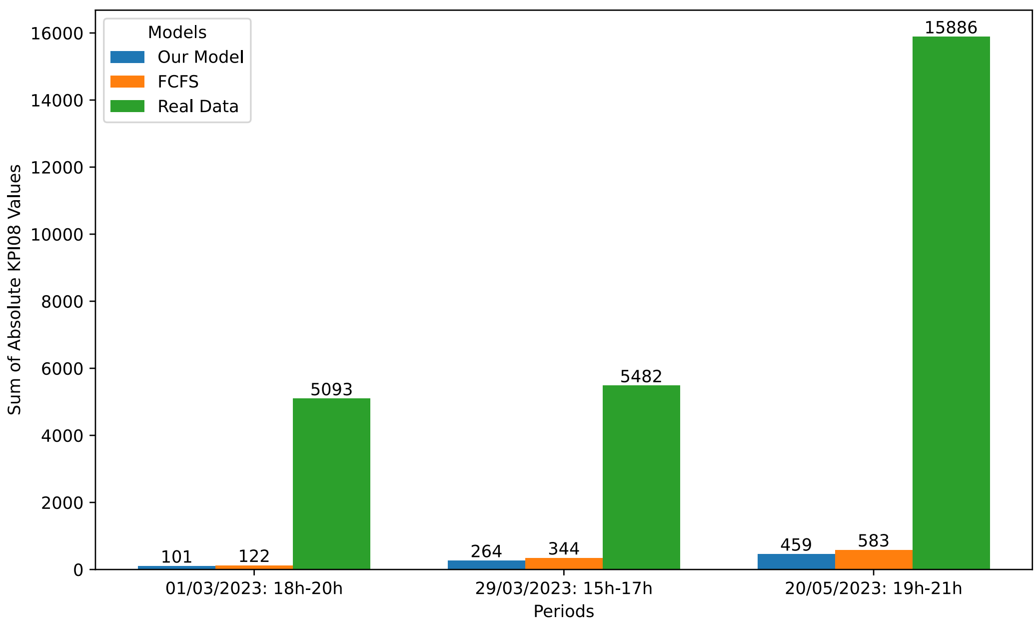

FIGURE 6.12 – Cumulative absolute KPI08 values for March 01, March 29, and May 20, 2023, in the C40 scenario.

In the threshold change scenario, the optimized model remains effective in reducing cumulative KPI08, achieving an average reduction of 20.58% compared to the FCFS baseline.

The real KPI08 values from BIMTRA are substantially higher, reflecting operational factors as discussed previously, with the added possibility of meteorological formations affecting landing sequences. Since our methodology did not account for weather conditions in data selection, this could contribute to the increased KPI08 values observed in real operations. Nevertheless, advance knowledge of runway threshold changes plays a critical role in reducing KPI08 values, as it enables sequencing adjustments to be made proactively, avoiding delays that would otherwise result from last-minute re-routing when a threshold change is unexpected.

Despite these real-world complexities, the optimized model demonstrates a remarkable improvement over BIMTRA's KPI08 values, achieving an average reduction of 96.77%.

6.4.2 C100 Scenario

The KPI08 comparison results for March 01, March 29, and May 20, 2023, in the C100 scenario with threshold change are displayed in Figures 6.13 to 6.15. As in the C40 scenario, aircraft landing sequences follow the FCFS baseline, with connecting lines illustrating order within each model. Figure 6.16 provides the cumulative absolute KPI08 values across the three days.

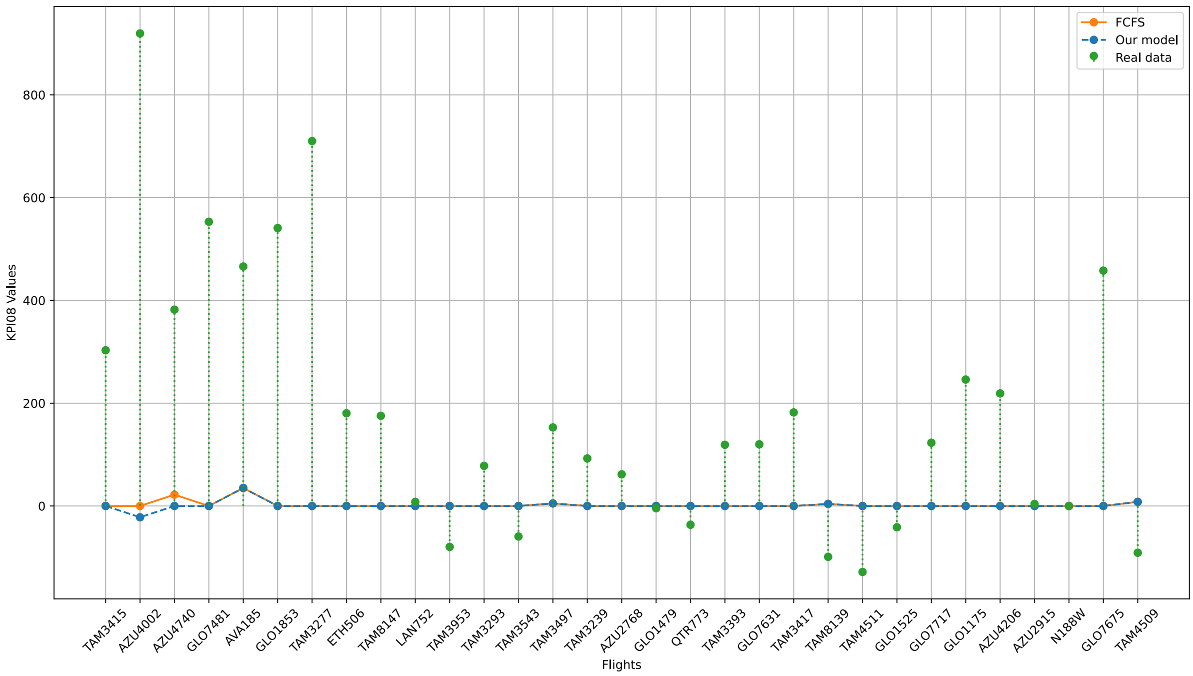

FIGURE 6.13 – KPI08 comparison for March 01, 2023, during the 18:00 to 20:00 period in the C40 scenario with threshold change.

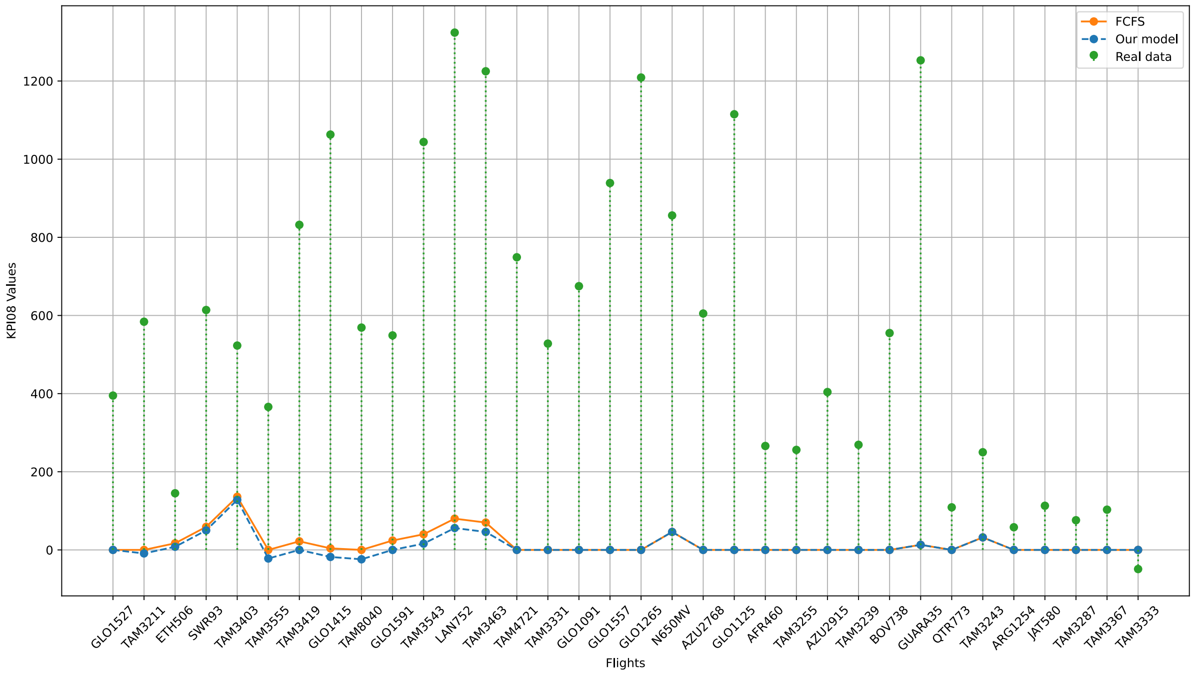

FIGURE 6.14 – KPI08 comparison for March 29, 2023, during the 15:00 to 17:00 period in the C100 scenario with threshold change.

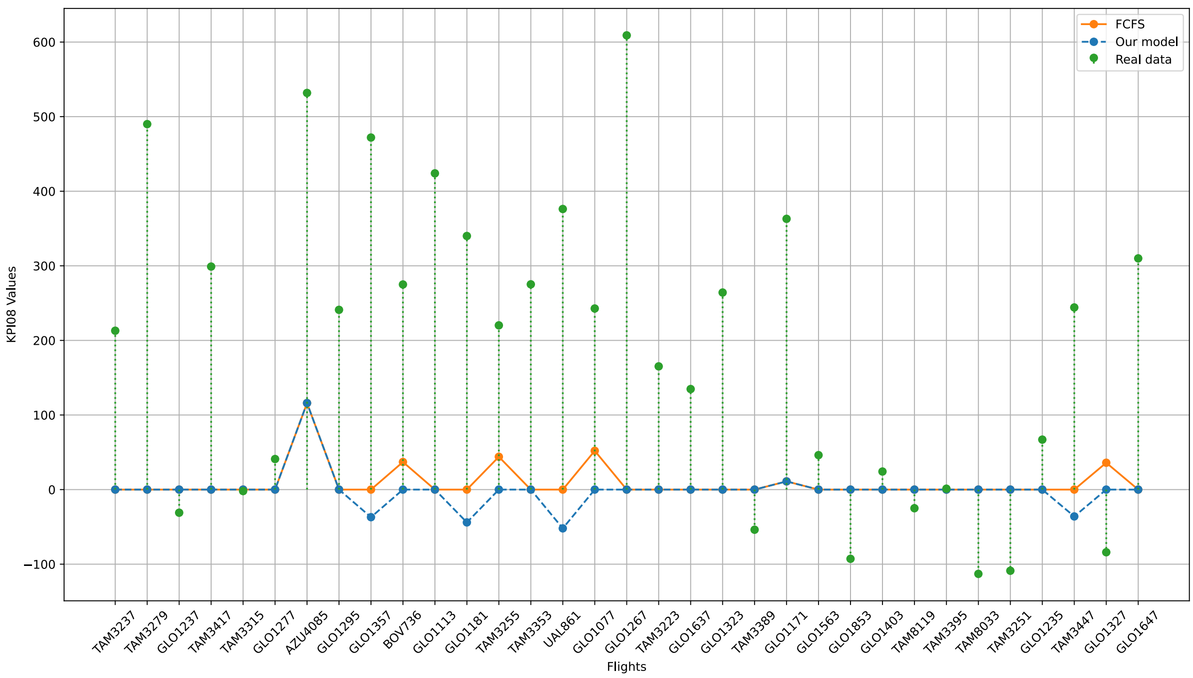

FIGURE 6.15 – KPI08 comparison for May 20, 2023, during the 19:00 to 21:00 period in the C100 scenario with threshold change.

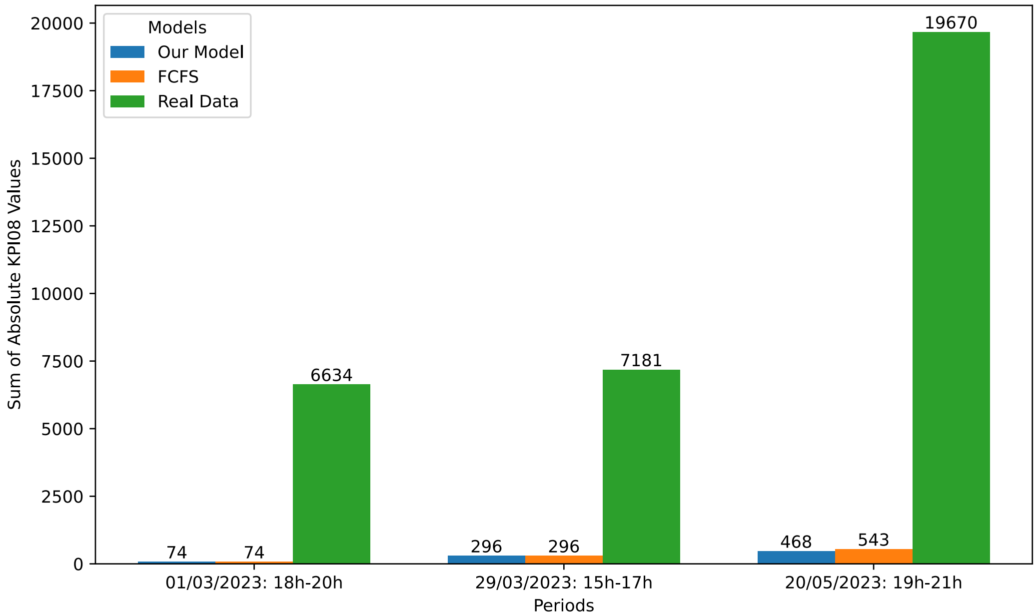

FIGURE 6.16 – Cumulative absolute KPI08 values for March 01, March 29, and May 20, 2023, in the C100 scenario.

In the C100 scenario with threshold change, the optimized model achieves a modest improvement over the FCFS baseline, with an average reduction of 4.60% in cumulative KPI08. This smaller difference is expected, as the larger airspace and typically greater spacing between arrivals in the C100 scenario limit the scope for sequencing adjustments. Furthermore, with landings occurring on two thresholds, the traffic for each threshold is reduced, which also lessens the potential for optimization gains. Additionally, the majority of flights in this scenario are medium-sized aircraft, resulting in a sequence that naturally aligns closely with the FCFS order. However, as shown in Figure 6.16, the optimized model achieves a maximum reduction of 98.89% over real KPI08 values from BIMTRA, highlighting its significant advantage over real operational conditions, despite the real-world complexities already discussed.

These results, combined with the findings from the C40 scenario, illustrate that the optimized model was also effective in reducing cumulative deviations in the threshold change scenario, although the improvement over FCFS was more modest. Nevertheless, both the optimized model and FCFS show substantial reductions in KPI08 compared to real-world BIMTRA data, underscoring the value of controlled, anticipatory sequencing. To more precisely determine how much of this improvement is attributable to advance knowledge of the runway change, further studies incorporating operational conditions and meteorological data would be necessary to fully understand the influence of these factors on KPI08 outcomes.

6.5 Efficacy Test in Busiest Days

The results from previous sections indicate that BIMTRA data presents significantly higher absolute KPI08 values compared to both the FCFS baseline and our optimized model. This suggests the influence of additional operational factors in real-world air traffic management that are not represented in the controlled simulation environment, making direct comparisons with BIMTRA data potentially unfair.

Given this discrepancy, we deemed it valuable to focus on high-traffic periods and compare our model's results directly with the FCFS baseline under peak conditions. By doing so, we can better assess the efficacy of our model relative to a straightforward sequencing approach, removing the complexities of real-world operations and focusing strictly on performance in high-density scenarios.

6.5.1 C40 Scenario

The comparison results for October 5, 2023, December 1, 2023, and September 13, 2023, each during the 10th hour, in the C40 scenario are shown in Figures 6.17 to 6.19. As in the previous sections, each figure displays KPI08 values for aircraft based on the FCFS baseline and the optimized model, with lines connecting the data points to represent the landing sequence determined by each approach. Figure 6.20 consolidates these results, showing the cumulative absolute KPI08 values across all three days.

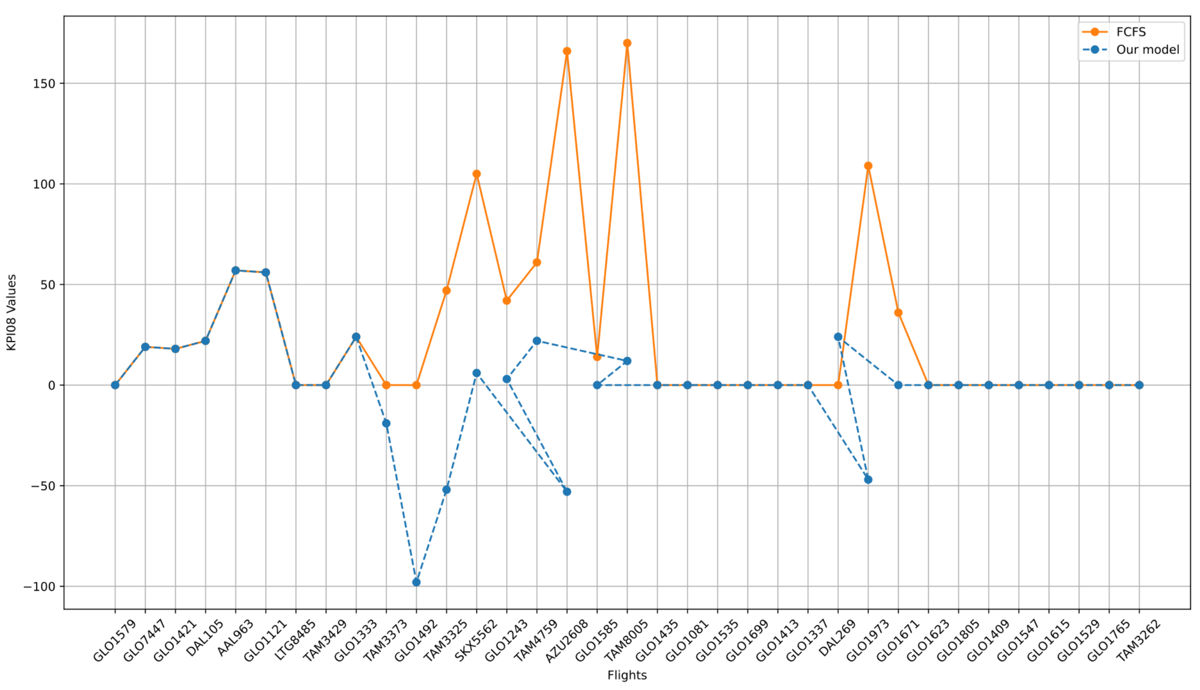

FIGURE 6.17 – KPI08 values for our model and FCFS model for the C40 scenario on October 5, 2023.

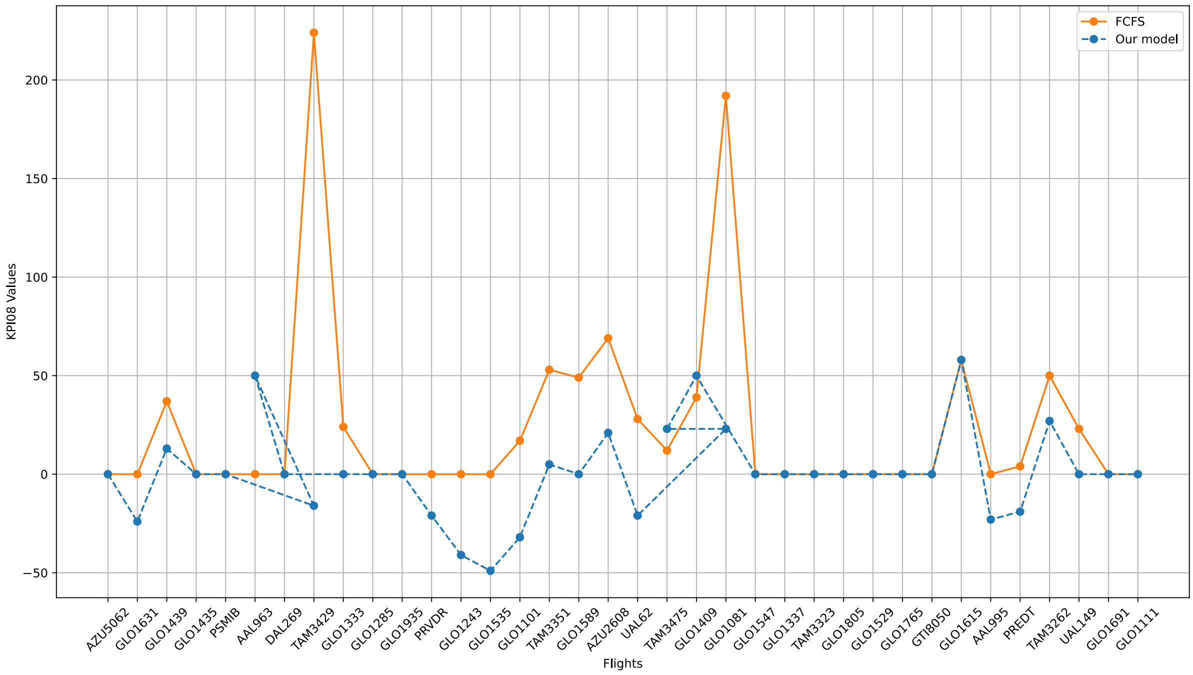

FIGURE 6.18 – KPI08 values for our model and FCFS model for the C40 scenario on September 13, 2023.

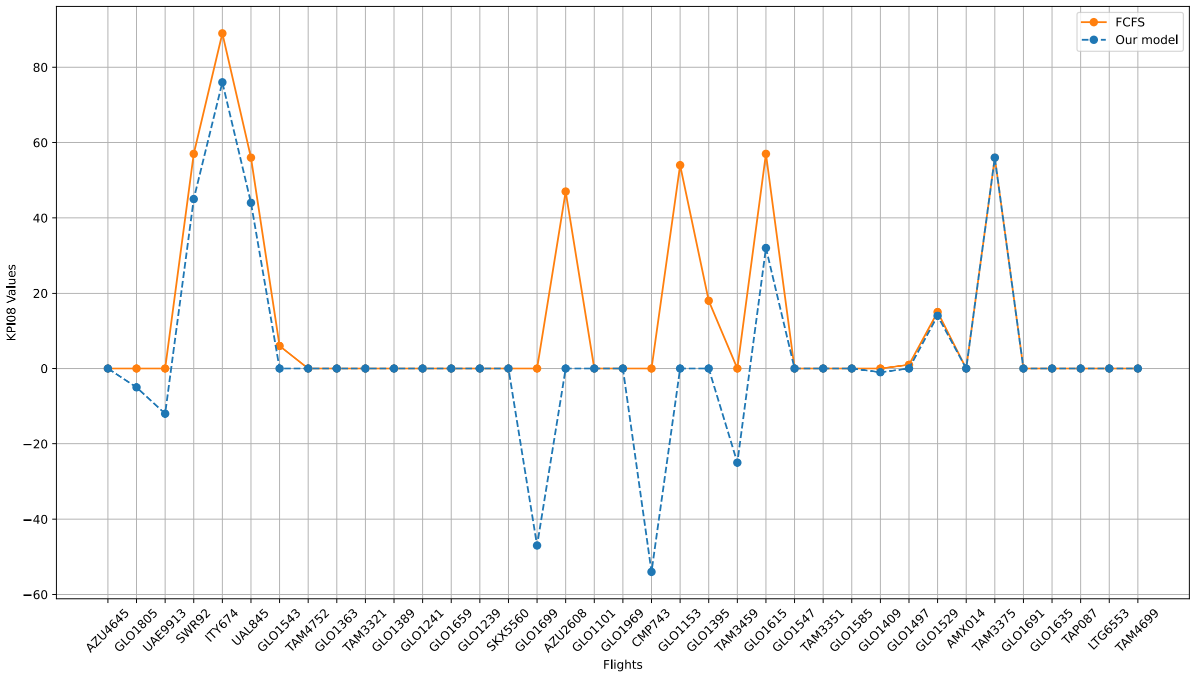

FIGURE 6.19 – KPI08 values for our model and FCFS model for the C40 scenario on December 1, 2023.

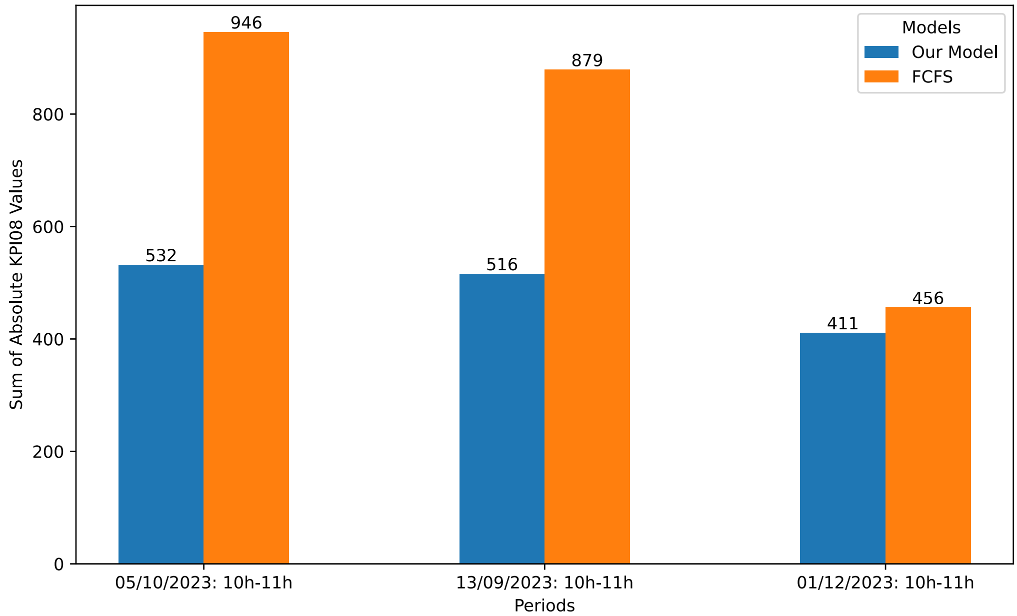

FIGURE 6.20 – Cumulative absolute KPI08 values for October 5, December 1, and September 13, 2023, in the C40 scenario.

In the C40 scenario, the optimized model achieved an average improvement of 31.64% in cumulative KPI08 compared to the FCFS baseline. This increase in the reductions compared to previous tests demonstrates that, under conditions of heavier traffic, the mathematical model can diverge more substantially from FCFS sequencing, taking advantage of optimization opportunities that are limited in less congested settings. Figures 6.17 and 6.18 illustrate the greater frequency of sequence adjustments, highlighting the optimized model's ability to reorder landings to reduce delays under high-traffic conditions. In contrast, Figure 6.19, demonstrates a more modest improvement in cases where no sequencing changes are made, underscoring the model's capacity to achieve KPI08 reductions both through reordering and precise timing adjustments.

6.5.2 C100 Scenario

The results for October 5, December 1, and September 13, 2023, each at the 10th hour in the C100 scenario, are illustrated in Figures 6.21 to 6.23. As previously, these figures display KPI08 values for aircraft according to both the FCFS baseline and the optimized model, with lines connecting data points to depict the landing sequence by each approach. Figure 6.20 provides an overall summary, presenting the cumulative absolute KPI08 values across the three days.

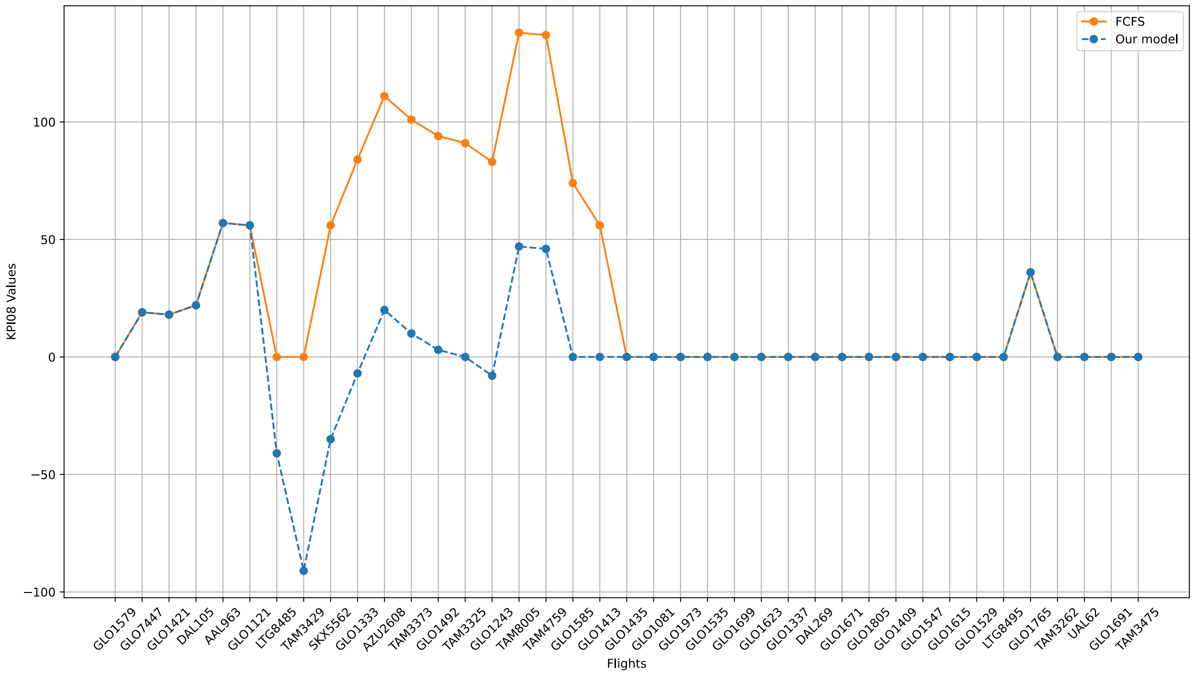

FIGURE 6.21 – KPI08 values for our model and FCFS model for the C100 scenario on October 5, 2023.

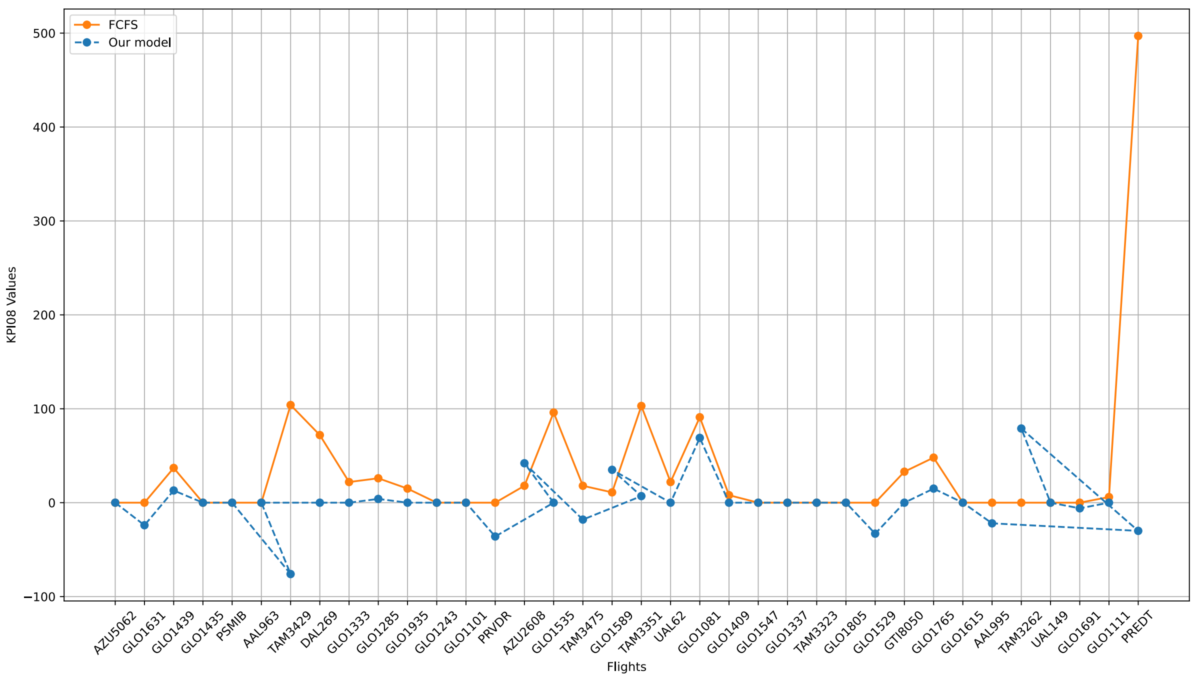

FIGURE 6.22 – KPI08 values for our model and FCFS model for the C100 scenario on September 13, 2023.

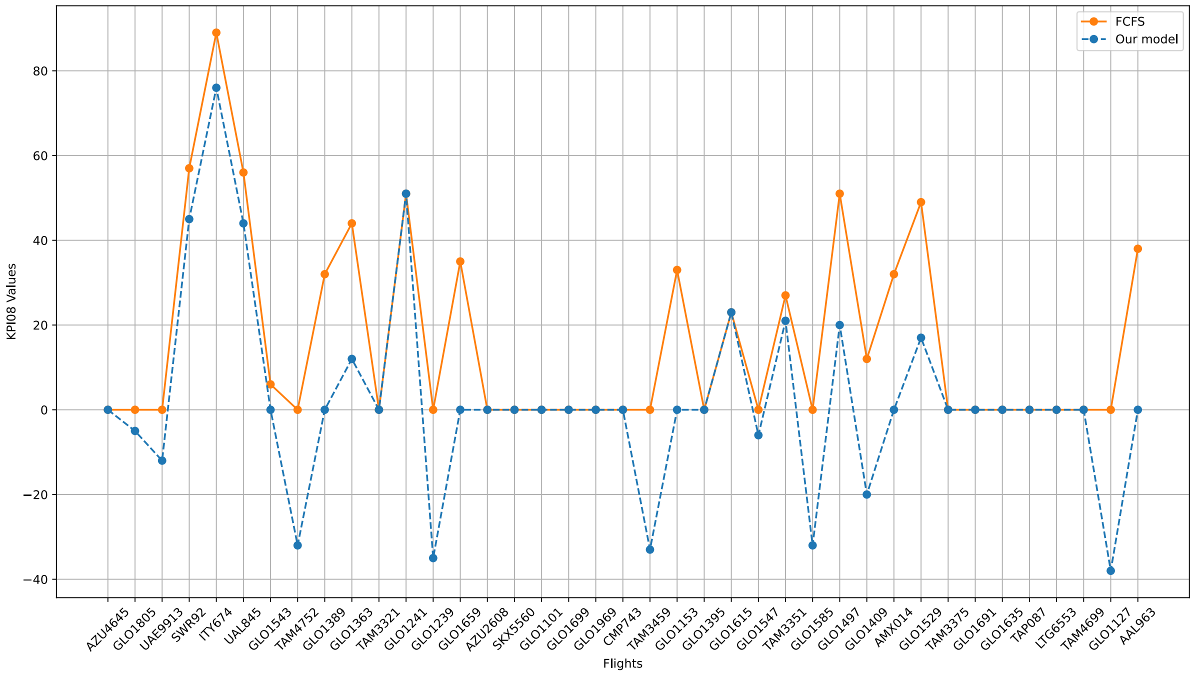

FIGURE 6.23 – KPI08 values for our model and FCFS model for the C100 scenario on December 1, 2023.

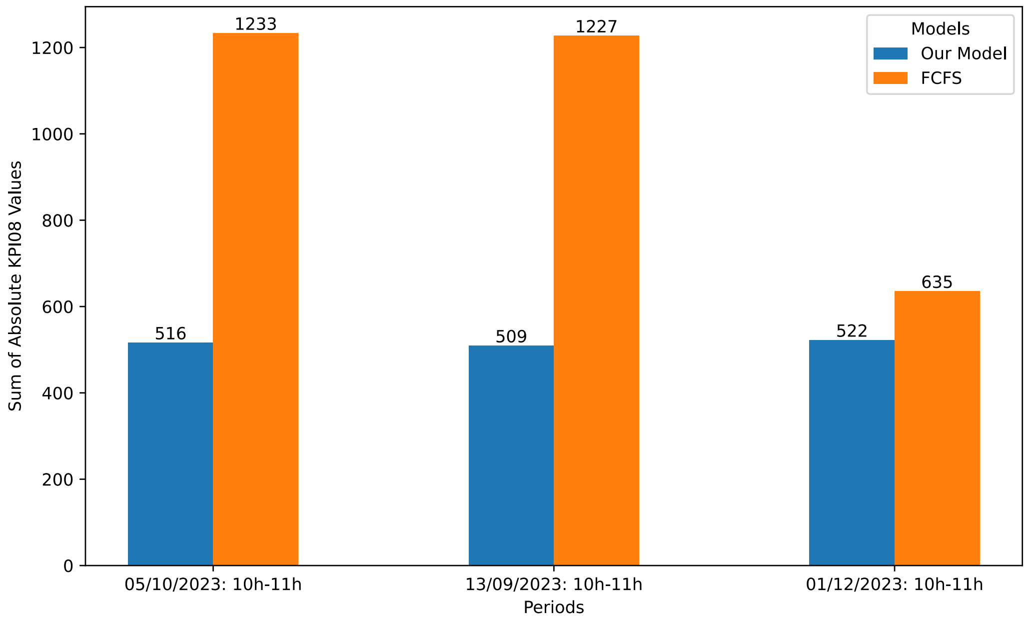

FIGURE 6.24 – Cumulative absolute KPI08 values for October 5, December 1, and September 13, 2023, in the C100 scenario.

In the C100 scenario, our optimized model exhibited an even more significant improvement over the FCFS baseline, achieving an average reduction of 45.37% in cumulative delays and advances. The most pronounced improvement was observed on September 13, with a maximum reduction of 60.15%, as illustrated in Figure 6.23. This larger airspace scenario includes a greater number of aircraft, which amplifies the potential benefits of sequencing optimizations. Despite the homogeneity in aircraft size, the expanded area provides more opportunities for the model to adjust arrival sequences effectively, leading to enhanced scheduling efficiency compared to the FCFS approach.

As illustrated in Figures 6.21 and 6.23, the two days with the highest number of sequencing changes also showed the greatest reductions relative to the FCFS baseline. Specifically, at the end of the day on September 13, it is notable that in the FCFS sequencing, the aircraft PREDT has a very high KPI08, while in the optimized sequencing, its KPI08 is much lower. This occurs because PREDT is a Light aircraft; if it lands after larger aircraft, it must maintain a greater distance, increasing its KPI08. Additionally, because it is smaller and slower, larger aircraft with earlier ETAs tend to overtake it, further increasing its wait time. In the optimized model, this issue is resolved by advancing PREDT in the sequence, resulting in a substantial reduction in the total absolute KPI08.

This significant improvement over the FCFS baseline during high-traffic days demonstrates the optimized model's effectiveness in reducing cumulative delays and advances, enabling aircraft to land closer to their initially expected times. Given that our model showed substantial gains over the FCFS baseline in an idealized simulation environment, it is expected to deliver similar improvements over real operational data in practical settings, helping to manage traffic more efficiently during peak periods.

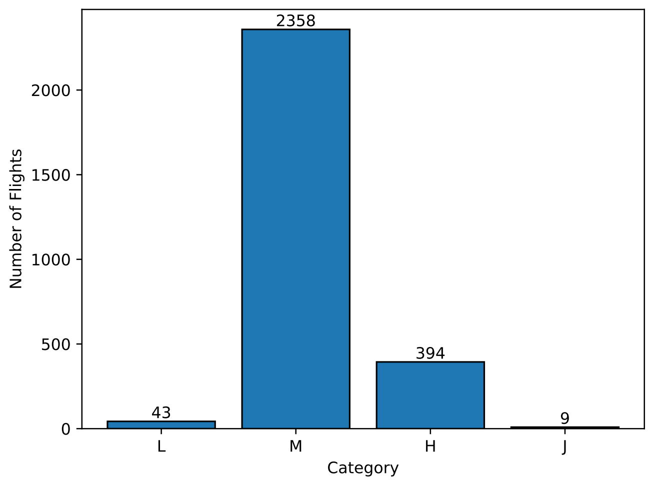

FIGURE 6.25 – Histogram of aircraft categories for the days analyzed in this study.

Overall, the optimized model consistently outperformed the BIMTRA data across all scenarios, demonstrating its robustness in reducing deviations from the unimpeded time. In nearly all cases the model also showed improvement over the FCFS baseline, with the exception of only two days in the threshold change scenario. Notably, these improvements were achieved even with a homogeneous mix of aircraft categories, where opportunities for sequencing adjustments are typically more limited.

To further illustrate this point, Figure 6.25 shows the histogram of flight categories on the nine days used in this study, highlighting the predominance of medium-sized aircraft with little variety. Even with this limited diversity, the model produced strong results, reinforcing its overall effectiveness and adaptability.

7 Conclusion and Future Work

In this chapter, we present the conclusion for the study and outline suggestions for future work.

7.1 Conclusion

This study successfully developed and implemented a computational model for optimizing aircraft sequencing at Guarulhos Airport, incorporating numerous operational constraints to closely reflect real-world conditions. Tested under various scenarios — including peak traffic periods — the model consistently demonstrated its ability to deliver viable solutions within efficient computation times.

The performance of the proposed model consistently exceeded that of the real-world data and almost always outperformed the FCFS baseline across all test instances. Notably, it matched the FCFS approach on two specific days involving threshold changes. This advantage was especially pronounced during high-traffic periods.

Moreover, the model shows significant promise for application in real-time air traffic management and serves as a solid foundation for the further development of AMAN systems. Its ability to adapt to various operational constraints suggests that it could play a crucial role in enhancing the efficiency and reliability of air traffic operations.

Looking ahead, as air traffic continues to grow and the mix of aircraft sizes becomes more diverse, the model's potential for optimization is expected to expand. A more populated airspace with a greater variety of aircraft provides additional opportunities for sequencing adjustments, which can lead to further reductions in deviations from unimpeded times.

In conclusion, this study establishes a robust basis for applying optimization techniques in air traffic management, showcasing the efficacy of a tailored computational model in addressing the complexities of high-demand airspace environments. The promising results highlight the model's potential to contribute to more efficient and reliable air traffic operations, particularly as the aviation industry continues to evolve.

7.2 Future Work

Future research could benefit from a deeper analysis of threshold changes, particularly by conducting tests in operational situations to understand how threshold adjustments impact sequencing efficiency. Evaluating the optimal advance notice for threshold changes could also shed light on how anticipation affects deviation minimization, allowing for more refined sequencing strategies under dynamic conditions.

Moreover, studies could investigate the effects of adjusting the weights assigned to delays and advances in the model's objective function. By varying these weights, future analyses could compare the trade-offs between delay minimization and fuel consumption, potentially developing sequencing strategies that balance efficiency with fuel savings and environmental impact.

Another promising research direction is the integration of heuristic methods to generate high-quality solutions within shorter time frames, especially for scenarios such as C100, which experience higher traffic density. As flight volumes continue to grow, the need for faster solution times will become crucial for maintaining efficiency in high-density airspaces.

Additionally, expanding the model to incorporate further phases of the AMAN system could enhance its applicability. For instance, integrating an arrival time predictor based on machine learning could significantly improve the accuracy of ETA calculations. By analyzing historical data and meteorological conditions, this predictive module would allow the model to adapt more effectively to real-time variables, ultimately improving overall model efficacy and enabling better decision-making in unpredictable scenarios.

Bibliography

ARENALES, M.; MORABITO, R.; YANASSE, H. **Pesquisa Operacional**. Rio de Janeiro: Elsevier Editora Ltda., 2007. ISBN 978-85-352-5193-7.

BALAKRISHNAN, H.; CHANDRAN, B. G. Algorithms for scheduling runway operations under constrained position shifting. **Operations Research**, INFORMS, v. 58, n. 6, p. 1650–1665, 2010.

BAZARAA, M. S.; JARVIS, J. J.; SHERALI, H. D. **Linear Programming and Network Flows**. 4th. ed. Hoboken, NJ: Wiley, 2005.

BEASLEY, J. E. Or-library: Distributing test problems by electronic mail. **Journal of the Operational Research Society**, Taylor & Francis, v. 41, n. 11, p. 1069–1072, 1990. Available at: https://doi.org/10.1057/jors.1990.166.

BEASLEY, J. E.; KRISHNAMOORTHY, M.; SHARAIHA, Y. M.; ABRAMSON, D. Scheduling aircraft landings—the static case. **Transportation Science**, v. 34, n. 2, p. 180–197, 2000. Available at: https://doi.org/10.1287/trsc.34.2.180.12302.

BEASLEY, J. E.; SONANDER, J.; HAVELOCK, P. Scheduling aircraft landings at london heathrow using a population heuristic. **Journal of the operational Research Society**, Taylor & Francis, v. 52, n. 5, p. 483–493, 2001.

BENCHEIKH, G.; BOUKACHOUR, J.; ALAOUI, A. E. H.; KHOUKHI, F. Hybrid method for aircraft landing scheduling based on a job shop formulation. **International Journal of Computer Science and Network Security**, v. 9, n. 8, p. 78–88, 2009.

BRISKORN, D.; STOLLETZ, R. Aircraft landing problems with aircraft classes. **Journal of Scheduling**, v. 17, n. 1, p. 31–45, 02 2014. ISSN 1099-1425. Available at: https://doi.org/10.1007/s10951-013-0337-x.

DECEA. **ICA 100-37: Serviços de Tráfego Aéreo**. [*S.l.*], 2020. Available at: https:/-/static.decea.mil.br/publicacoes/files/2020/a4480c0a-3657-4ba0-87721154264d0766.pdf.

DECEA. **MCA 100-22: Metodologia de Indicadores ATM do SISCEAB**. [*S.l.*], 2020. Available at: https://www.icao.int/SAM/Documents/2021-RLA06901-TallerVOLIII-1/BRASIL%20%20MCA%20100-22.pdf.

EUROCONTROL. **Challenges of Growth 2018**. 2018. `https://www.eurocontrol.int/publication/challenges-growth-2018`.

FAHLE, T.; FELDMANN, R.; GÖTZ, S.; GROTHKLAGS, S.; MONIEN, B. The aircraft sequencing problem. *In*: _____. **Computer Science in Perspective: Essays Dedicated to Thomas Ottmann**. Berlin, Heidelberg: Springer Berlin Heidelberg, 2003. p. 152–166. ISBN 978-3-540-36477-1. Available at: https://doi.org/10.1007/3-540-36477-3_11.

FAYE, A. Solving the aircraft landing problem with time discretization approach. **European Journal of Operational Research**, Elsevier, v. 242, n. 3, p. 1028–1038, 2015.

GHONIEM, A.; FARHADI, F. A column generation approach for aircraft sequencing problems: a computational study. **Journal of the Operational Research Society**, Taylor & Francis, v. 66, n. 10, p. 1717–1729, 2015.

HANCERLIOGULLARI, G.; RABADI, G.; AL-SALEM, A. H.; KHARBECHE, M. Greedy algorithms and metaheuristics for a multiple runway combined arrival-departure aircraft sequencing problem. **Journal of Air Transport Management**, Elsevier, v. 32, p. 39–48, 2013.

ICEA. **Informação sobre mudança de cabeceira para o Aeroporto Internacional de Guarulhos**. 2023. `https://pesquisa.icea.decea.mil.br/read_cabeceira/?csrfmiddlewaretoken=ZwcoVxaEvf6lKoXpPQlcIOwxMRWtw9zXcU1zOC4LoCRgihnZGZKrKDg2yJSMQqm3&tf_search_station=SBGR`.

IKLI, S.; MANCEL, C.; MONGEAU, M.; OLIVE, X.; RACHELSON, E. The aircraft runway scheduling problem: A survey. **Computers & Operations Research**, v. 132, p. 105336, 2021. ISSN 0305-0548. Available at: https://www.sciencedirect.com/science/article/pii/S0305054821001192.

LUENBERGER, D. G.; YE, Y. **Linear and Nonlinear Programming**. 3rd. ed. New York: Springer, 2008.

PRAKASH, R.; PIPLANI, R.; DESAI, J. An optimal data-splitting algorithm for aircraft scheduling on a single runway to maximize throughput. **Transportation Research Part C: Emerging Technologies**, Elsevier, v. 95, p. 570–581, 2018.

SILVA, L. C. d.; UENO, F. Y.; SANTOS, M. O. d.; CARVALHO, A. C. P. d. L. F. d. A new modelling for the aircraft landing problem and matheuristic approach to solve the problem with a large number of aircraft. **Pesquisa Operacional**, Sociedade Brasileira de Pesquisa Operacional, v. 43, p. e266290, 2023. ISSN 0101-7438. Available at: https://doi.org/10.1590/0101-7438.2023.043.00266290.

Skybrary. **Arrival Manager (AMAN)**. 2024. `https://skybrary.aero/articles/arrival-manager-aman`.

SOARES, I. B.; HAUWERE, Y.-M. D.; JANUARIUS, K.; BRYS, T.; SALVANT, T.; NOWÉ, A. Departure management with a reinforcement learning approach: Respecting cfmu slots. *In*: IEEE. **2015 IEEE 18th International Conference on Intelligent Transportation Systems. Proceedings** [...]. [*S.l.: s.n.*], 2015. p. 1169–1176.

SOOMER, M. J.; FRANX, G. J. Scheduling aircraft landings using airlines' preferences. **European Journal of Operational Research**, Elsevier, v. 190, n. 1, p. 277–291, 2008.

STEVENS, G. An approach to scheduling aircraft landing times using genetic algorithms. **RMIT: Department of Computer Science**, 1995.

VERESNIKOV, G.; EGOROV, N. A.; KULIDA, E. L.; LEBEDEV, V. G. Methods for solving of the aircraft landing problem. i. exact solution methods. **Automation and Remote Control**, Springer, v. 80, p. 1317–1334, 2019.

VERESNIKOV, G.; EGOROV, N. A.; KULIDA, E. L.; LEBEDEV, V. G. Methods for solving of the aircraft landing problem. ii. approximate solution methods. **Automation and Remote Control**, Springer, v. 80, p. 1502–1518, 2019.

FOLHA DE REGISTRO DO DOCUMENTO

1. CLASSIFICAÇÃO/TIPO	2. DATA	3. DOCUMENTO Nº	4. Nº DE PÁGINAS
TC	22 de novembro de 2024	DCTA/ITA/TC-109/2024	84

5. TÍTULO E SUBTÍTULO:

Optimization of Aircraft Sequencing Using Mixed-Integer Programming

6. AUTOR(ES):

Victor Maciel

7. INSTITUIÇÃO(ÕES)/ÓRGÃO(S) INTERNO(S)/DIVISÃO(ÕES):

Instituto Tecnológico de Aeronáutica – ITA

8. PALAVRAS-CHAVE SUGERIDAS PELO AUTOR:

Aircraft Landing Problem; Arrival Manager; Mixed-Integer Programming.

9. PALAVRAS-CHAVE RESULTANTES DE INDEXAÇÃO:

Pesquisa operacional; Métodos heurísticos; Controle de tráfego aéreo; Aterrissagem; Decolagem; Otimização; Matemática; Transportes.

10. APRESENTAÇÃO: (**X**) **Nacional** ( ) **Internacional**

ITA, São José dos Campos. Curso de Graduação em Engenharia de Computação. Orientador: Prof. Dr. Carlos Henrique Costa Ribeiro. Coorientador: Prof. Dr. Luís Felipe Bueno. Publicado em 2024.

11. RESUMO:

The rapid growth in global air travel demand has significantly increased air traffic, leading to heightened delays and environmental concerns. This surge underscores the critical need for optimized sequencing techniques in air traffic management to maintain operational efficiency. Operational Research provides powerful methods to tackle these complex issues by offering structured approaches for optimization. In this study, we develop a Mixed-Integer Programming model to address the Aircraft Landing Problem, incorporating operational constraints specific to Guarulhos International Airport. Our model aims to enhance the efficiency of aircraft landing sequences by minimizing cumulative deviations from unimpeded times, thereby reducing fuel consumption and improving overall airport performance. To assess the model's viability and efficacy, we employed a data-driven approach, collecting real operational data from Guarulhos International Airport during select days in 2023. This approach enabled us to evaluate the model under various traffic scenarios, including those involving threshold changes. The results indicate that our model's implementation consistently achieved viable solutions with practical execution times and outperformed both actual operational data and the First-Come, First-Served (FCFS) baseline regarding deviations from unimpeded times. Under clear visibility and moderate traffic conditions, the model showed an average improvement of 93.33% over real data and 29.91% over the FCFS baseline. In peak traffic scenarios, it demonstrated a maximum improvement of 60.15% compared to FCFS when optimization began at 100 nautical miles (NM) from the airport, with an average improvement of 45.37% across the analyzed days. When optimization began at 40 NM from the airport, the model achieved an average improvement of 31.64% over FCFS. Similar gains were observed in scenarios involving threshold changes. These findings demonstrate the model's potential as a robust tool for optimizing landing sequences, contributing to reduced deviations from unimpeded times and environmental impact, while enhancing overall airport efficiency.

12. GRAU DE SIGILO:

(**X**) **OSTENSIVO** ( ) **RESERVADO** ( ) **SECRETO**